Amidoboranes and hydrazinidoboranes: State of the art, potential for hydrogen storage, and other prospects

Carlos A. Castilla-Martinez, Romain Moury, Umit B. Demirci

Amidoboranes and hydrazinidoboranes: state of the art, potential for hydrogen storage, and other prospects

Carlos A. CASTILLA-MARTINEZ [a], Romain MOURY [b], Umit B. DEMIRCI [a,*]

[a] Institut Européen des Membranes, IEM – UMR 5635, ENSCM, CNRS, Univ Montpellier, Montpellier, France

[b] Institut des Molécules et Matériaux du Mans, University of Le Mans, Avenue Olivier Messiaen, Le Mans, 72085, France

* umit.demirci@umontpellier.fr

Abstract

Following the seminal B-N-H compound ammonia borane NH_3BH_3, a series of derivatives have been developed as possible chemical hydrogen carriers. First, alkali and alkaline earth derivatives of ammonia borane, i.e. amidoboranes $M(NH_2BH_3)_n$ with n = 1 or 2, emerged. Then, hydrazine borane, which is actually a derivative of ammonia borane, was re-discovered and considered as a precursor of alkali and alkaline earth derivatives, i.e. hydrazinidoboranes $M(N_2H_3BH_3)_n$. A number of B-N-H ionic salts were, in this way, synthesized and reported. The present review provides the general background (e.g. syntheses, crystallographic structures, thermal stability, dehydrogenation properties, and decomposition mechanisms) relating to these alkali and alkaline earth amidoboranes and hydrazinidoboranes, and carries on two objectives. The first objective is to discuss the potential of these materials (for the application for which they have been primarily developed over the past decades, namely hydrogen storage) and the challenges they are facing. It is concluded that the light alkali amidoboranes, namely the lithium, sodium and potassium amidoboranes) should be further developed owing to better dehydrogenation properties in terms of the onset temperature of dehydrogenation, the extent of dehydrogenation, and the purity of the hydrogen released. They should, however, be further developed with the aim of upscaling, something that has not yet been achieved. Achieving high technological readiness levels is thereby the main challenge ahead. The second objective of the present review is to explore alternative uses because, as things stand, none of the developed materials have the expected features for hydrogen storage. We suggest that any of the discussed derivatives are potentially solid-state reducing agents, energetic materials, and/or precursors of boron nitride-based ceramics, bearing in mind that for this last use, if the targeted material is porous, it could be regarded as a reversible hydrogen sorbent. It is thus important to maintain efforts in the development of the current derivatives as well as in the discovery of novel ones.

Keywords

Amidoborane; Ammonia borane; Hydrazine borane; Hydrazinidoborane; Hydrogen storage.

1. Introduction

Dihydrogen H_2 is highly energetic, at least gravimetrically (142 MJ kg^{-1}). It could have been an excellent alternative to oil (more broadly to fossil fuels) if it was extensively available in accessible natural reserves and if it was a gas. This is not the case. Dihydrogen has to be produced from sources carrying elemental hydrogen, and it has to be stored to improve its volumetric energy capacity (>>12.7 kJ L^{-3}). Accordingly, a great deal of effort has gone into developing efficient and cost-effective methods for producing, storing, and converting (i.e. fuel cell technology) H_2 [1-3].

Storing H_2 is not an easy task. Beyond the conventional methods that are pressurization and liquefaction in cryogenic conditions [4-6], a number of new approaches have emerged and been developed within the past twenty years. These approaches are based on storing H within a liquid and/or a solid [7-9]. In the solid state, two strategies have been developed. The first one is based on the physical interactions between H_2 and the surface of a porous material (e.g. carbonaceous, metal organic frameworks, polymers) [10]. The second, is based on the binding properties (chemical or physicochemical interactions) between H and a heteroelement like an alkaline earth metal (e.g. Mg) [11], a metal (e.g. Ni) [12], a metalloid (e.g. B) [13], and a non-metal (e.g. the p-block element N) [14].

In the metalloid B category, whether combined or not with the element N, a great number of B-(N-)H compounds, showing high gravimetric and volumetric H densities, have been synthesized and studied as chemical hydrogen storage materials [15]. However, these H carriers offer limited or no reversibility in terms of H_2 storage. With this regard, the challenge with such materials is to find the best and most efficient paths for high-extent dehydrogenation.

The first example belonging to the borohydrides family (i.e. B-H compounds) is sodium borohydride $NaBH_4$ which carries 10.65 wt. % H [16]. At ambient conditions, the hydridic hydrogens $H^{\delta-}$ of the anion BH_4^- are able to react spontaneously and exothermically with protic hydrogens $H^{\delta+}$ of water. Hydrolysis takes place [17]. Via such a reaction, half of the evolving H_2 is due to BH_4^- and the other half to four equivalents of H_2O:

$$NaBH_4 + 4H_2O \rightarrow NaBO_2 \cdot 2H_2O + 4H_2 \quad (1)$$

A metal-based heterogeneous catalyst accelerates the reaction [18]. Alternatively, $NaBH_4$ can be dehydrogenated by thermolysis, but the reaction has sluggish kinetics and requires high temperatures (>500 °C) [19]. Better dehydrogenation properties can be achieved through chemical modification implying e.g. a second cation like Zn^{2+} [20].

The second example belonging to the family of amine-boranes (i.e. B-N-H compounds) is ammonia borane NH_3BH_3 (AB). It is isoelectronic with ethane C_2H_6, and carries six hydrogen elements that account for a gravimetric H density of 19.6 wt. % [21]. Precisely, it carries three $H^{\delta+}$ in the NH_3 group and three $H^{\delta-}$ in the BH_3 moiety. The existence of these two types of H, and implicitly of intermolecular dihydrogen $H^{\delta+}\cdots H^{\delta-}$ interactions [22], rationalizes the solid state of the compound [23] and its ability to dehydrogenate under moderate conditions starting around 100 °C [24]. Consequently, thermal dehydrogenation of AB has been widely investigated [25]. However, pristine AB does not only dehydrogenate, it decomposes into gaseous species like ammonia NH_3, diborane B_2H_6 and borazine $B_3N_3H_6$ and into a B-N-H residue of complex composition (Figure 1). This paved the way to the development of destabilization strategies allowing pure dehydrogenation [26]. Among the strategies envisaged so far, is the synthesis of derivatives via substitution of one $H^{\delta+}$ by a metal cation, for instance lithium amidoborane $LiNH_2BH_3$ [27]. AB has also been investigated for H_2 release by hydrolysis [28] despite the drawbacks connected with the NH_3 group (i.e. pollution of the H_2 stream by evolution of some NH_3, and impossible dehydrogenation of NH_3 in hydrolysis conditions) [29].

Another B-N-H compound of interest is hydrazine borane $N_2H_4BH_3$ (HB; 15.4 wt. % H) [30], a derivative of AB where the N_2H_4 group replaces NH_3. On the one hand, HB has been studied for dehydrogenation in hydrolytic medium [31]. More attractive than AB, it is able to dehydrogenate, not only by hydrolysis of the BH_3 moiety but also by dehydrogenation of the N_2H_4 group [32]:

$$N_2H_4BH_3 + 4H_2O \rightarrow B(OH)_3 + N_2 + 5H_2 \quad (2)$$

In the presence of an active and selective nickel-based catalyst, a total dehydrogenation of aqueous HB (with co-formation of N_2 and $B(OH)_3$) was achieved [33]. On the other hand, HB has been investigated for dehydrocoupling in thermolysis conditions [30], even though it is not suitable: it predominantly decomposes into the unwanted N_2H_4 and generates a shock-sensitive solid when the temperature exceeds 300 °C (Figure 1). Alternatively, like for AB, substitution of

$H^{\delta+}$ by an alkali cation has also been explored leading to metal hydrazinidoboranes, for instance lithium hydrazinidoborane $LiN_2H_3BH_3$ [34].

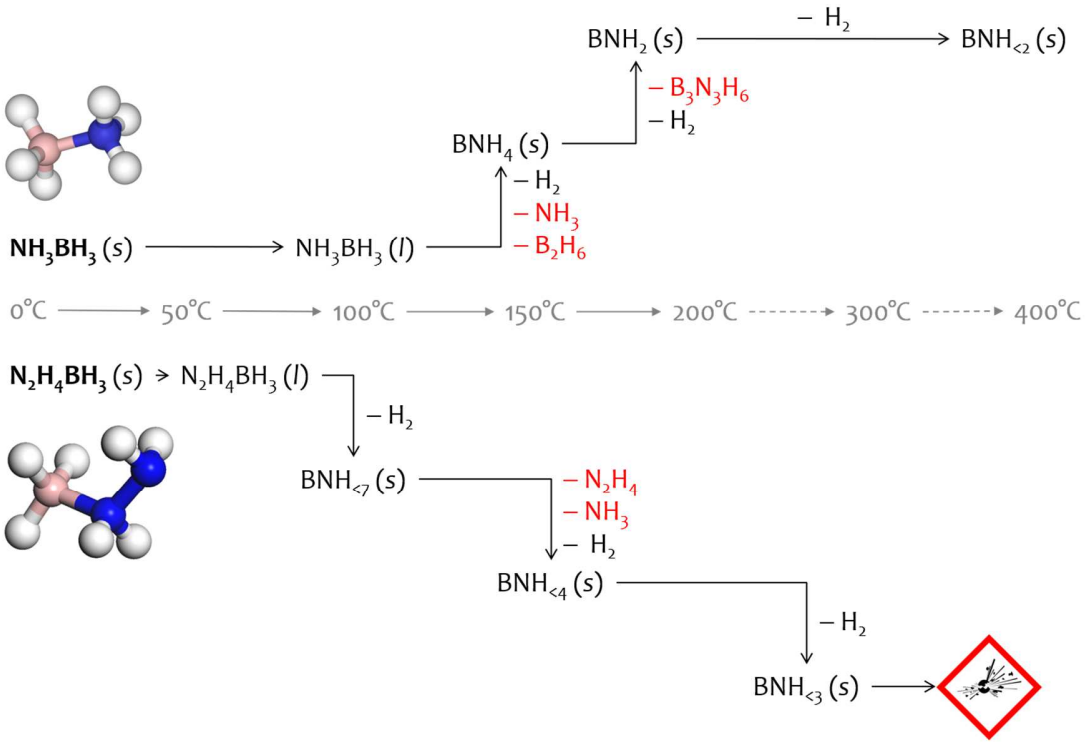

Figure 1. Schematized representation of thermal decomposition of pristine AB and pristine HB within the temperature range 0-400 °C. Because the thermolysis residues forming after each decomposition are of complex (rather unknown) composition, they are represented by BNH_x (with x = <2, 2, <3, <4, 4, <7). The pictograms represent the volatile by-products as well as, for decomposed HB, a shock-sensitive solid.

Both AB and HB have spawned new B-N-H compounds, specifically amidoboranes and hydrazinidoboranes. These derivatives have better dehydrogenation properties than the parent boranes. Interestingly, amidoboranes and hydrazinidoboranes are comparable in some aspects but different in others. The present article focuses on such alkali and alkaline earth derivatives. It aims at making a survey of the similarities as well as of the main differences. It is concluded that we do not know amidoboranes and hydrazinidoboranes well enough and that further efforts, particularly focusing on upscaling, are required to better understand them. It is also concluded that the most suitable compounds for hydrogen storage appear to be the lithium, sodium and potassium amidoboranes. Amidoboranes should be preferred to hydrazinidoboranes because the

latter derivatives decompose into ammonia and/or hydrazine. The present article also aims at putting their application potential into perspective. The current knowledge and understanding of amidoboranes and hydrazinidoboranes have made three other utilizations emerge. These materials have prerequisites to be used as solid-state reducing agents, energetic materials, and/or precursors of boron nitride-based ceramics. This is discussed in detail herein.

2. Preamble about amidoboranes

The first report about an amidoborane dates from the 1940s. The sodium compound $NaNH_2BH_3$ was synthesized through a two-step process [35,36]:

$$(CH_3)_2O{\cdot}BH_3 + 2NH_3 \rightarrow [BH_3NH_2]^-[NH_4]^+ + (CH_3)_2O \quad (3a)$$

$$[BH_3NH_2]^-[NH_4]^+ + Na(Hg) \rightarrow NaNH_2BH_3 + NH_3 + 1/2H_2 \quad (3b)$$

About sixty years later, the lithium counterpart $LiNH_2BH_3$ was reported [37]. It was successfully synthesized by using AB as precursor and THF as solvent:

$$NH_3BH_3 + C_4H_9Li \rightarrow LiNH_2BH_3 + C_4H_{10} \quad (4)$$

$LiNH_2BH_3$ is a highly nucleophilic reducing agent used for the transformation of tertiary amides into primary alcohols. However, it was not until 10 years later, in the second half of the 2000s, that amidoboranes began to flourish.

The first metal amidoborane of the third millennium, also the first proposed as a potential hydrogen storage material, is calcium amidoborane $Ca(NH_2BH_3)_2$. It was synthesized according to a two-step process [38]. AB and calcium hydride CaH_2 were reacted in THF resulting in a bis(thf) adduct:

$$2NH_3BH_3 + CaH_2 + 2THF \rightarrow Ca(thf)_2(NH_2BH_3)_2 + 2H_2 \quad (5)$$

Most of the coordinated THF molecules, but not all, were removed under vacuum. Upon heating, the remaining THF desorbed at about 70 °C. Like the parent AB, $Ca(NH_2BH_3)_2$ dehydrogenates above 100 °C, but unlike AB, it offers some advantages. The amidoborane releases cleaner H_2 (polluted by less than 0.1 wt. % of NH_3 and $B_3N_3H_6$); it does not show an induction period in isothermal conditions; it does not foam; its dehydrogenation extent is higher than 2 equiv H_2; and, the dehydrogenation process is less exothermic [38,39].

The re-discovery of both $LiNH_2BH_3$ and $NaNH_2BH_3$ primarily confirmed the potential of amidoboranes [27]. They, together with other alkali (K, Rb, Cs) and alkaline earth (Be, Mg, Ca, Sr, Ba) derivatives, are discussed in detail in the next sections. Particularly, they are compared to hydrazinidoboranes based on the same cations. Figure 2 shows all of these B-N-H compounds, and their respective gravimetric hydrogen density (in wt. % H) is given.

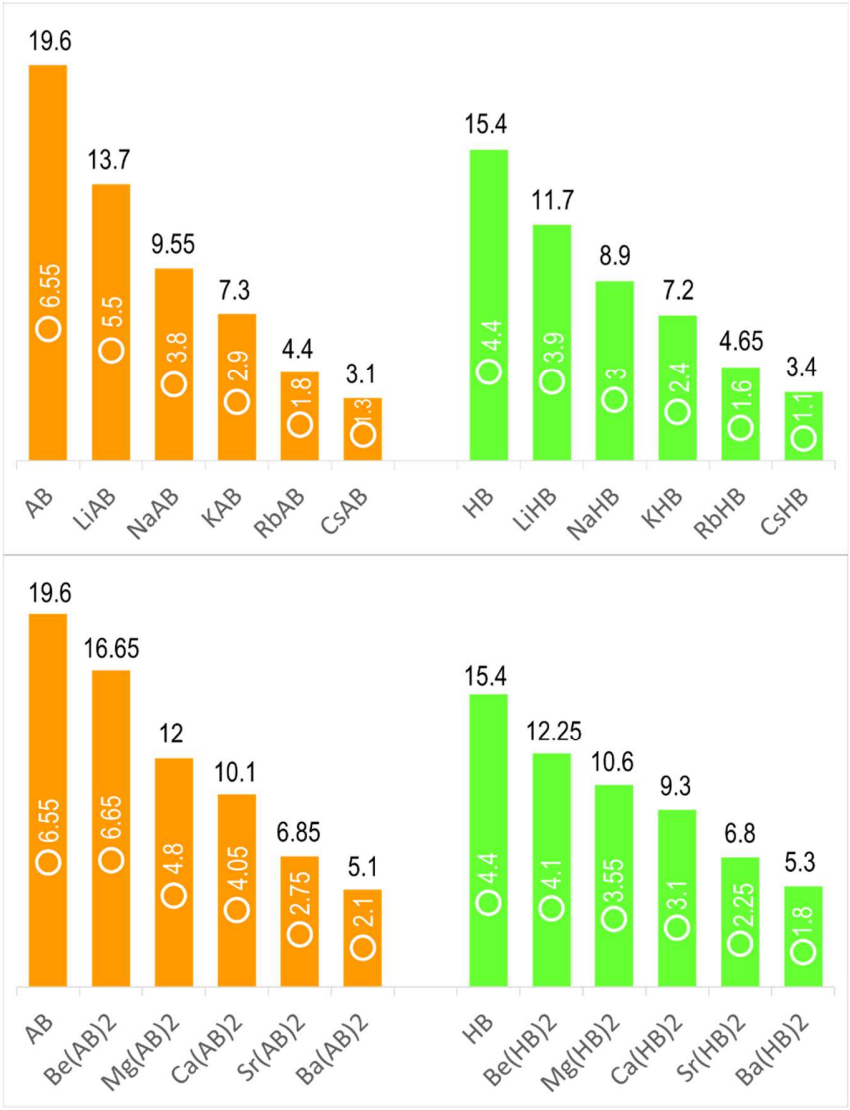

Figure 2. Gravimetric hydrogen densities (in wt. % H) for AB and HB, MAB and MHB (with M = Li, Na, K, Rb, Cs; top figure), and $M(AB)_2$ and $M(HB)_2$ (with M = Be, Mg, Ca, Sr, Ba; bottom figure). The bars and the black numbers on the top of each bar represent the theoretical values. The circles inside the bars and the white numbers inside each bar represent the effective gravimetric hydrogen storage capacities.

The demonstrated potential of both $LiNH_2BH_3$ and $NaNH_2BH_3$ gave a glimpse of the potential of new amidoboranes. A first example is $LiNH_2BH_3{\cdot}NH_3BH_3$ prepared by reacting $LiNH_2BH_3$ and NH_3BH_3 in a molar ratio 1:1 or LiH and NH_3BH_3 in a ratio 1:2 [40]. $LiNH_2BH_3{\cdot}_3BH_3$ melts at 58 °C (vs 82 °C for $LiNH_2BH_3$ and 95 °C for AB) and concomitantly starts to release H_2. Theoretical calculations showed that the lower stability of $LiNH_2BH_3{\cdot}NH_3BH_3$ as compared to $LiNH_2BH_3$ is due to weakened $B{-}H^{\delta-}{\cdots}H^{\delta+}{-}N$ interactions [41]. Ammonia NH_3 is also a possible ligand giving then, $LiNH_2BH_3{\cdot}NH_3$ [42]. Two other ammoniate amidoboranes are $Mg(NH_2BH_3)\cdot xNH_3$ (x = 1, 2) and $Ca(NH_2BH_3)\cdot 2NH_3$ [43-45]. Another ligand is hydrazine N_2H_4, giving the derivatives $LiNH_2BH_3{\cdot}N_2H_4$ and $Ca(NH_2BH_3)\cdot xN_2H_4$ (x = 0.5, 1, 2) [46,47].

Heavy cations like Y^{3+} were also considered. Yttrium amidoborane $Y(NH_2BH_3)_3$ was obtained by milling $LiNH_2BH_3$ and yttrium chloride YCl_3 [48]. It is unstable at ambient conditions and decomposes. Two other examples are: aluminum amidoborane $Al(NH_2BH_3)_3$ which, however, was contaminated with some MCl (M = Li, Na, K) [49,50], and zinc amidoborane $Zn(NH_2BH_3)_2$ which was synthesized at temperatures lower than −30 °C because of its instability [51,52].

Efforts were dedicated to other amidoboranes. In comparison with what was done before with mixed-cation borohydrides [53], bimetallic amidoboranes were synthesized [54-69]: $LiAl(NH_2BH_3)_4$, $Li_2Mg(NH_2BH_3)_4$, $NaLi(NH_2BH_3)_2$, $NaMg(NH_2BH_3)_3$, $Na_2Mg(NH_2BH_3)_4$, $NaAl(NH_2BH_3)_4$, $KMg(NH_2BH_3)_3$, $KAl(NH_2BH_3)_4$, $K_2Mg(NH_2BH_3)_4$, and $RbMg(NH_2BH_3)_3$. Otherwise, methyl-substituted amidoboranes like $LiN(CH_3)_2BH_3$ [70], and organometallic-complexed amidoboranes like $(\eta^5\text{-}C_5H_5)_2Zr(H)NH_2BH_3$ were considered [71]. Details about these other amidoboranes can be found in several review articles [72-77].

3. Alkali amidoboranes and hydrazinidoboranes

3.1. About AB and HB

AB (tetragonal, s.g. *I*4*mm* [78]) and HB (orthorhombic, s.g. *Pbcn* [79]) have several features in common. First, they are synthesized following a similar pathway (metathesis followed by

dehydrogenation) using $NaBH_4$ and an ammonium/hydrazinium salt in an organic solvent like THF or dioxane, at 30-40 °C [79,80]. For instance:

$$NaBH_4 + NH_4Cl \rightarrow NH_3BH_3 + H_2 + NaCl \quad (6)$$

$$NaBH_4 + N_2H_4 \cdot 1/2H_2SO_4 \rightarrow N_2H_4BH_3 + H_2 + 1/2Na_2SO_4 \quad (7)$$

Second, AB and HB are solid at ambient conditions. Third, they show comparable stability under argon atmosphere, under air and in organic/protic solution [24-26,34]. Fourth, both of them are unsuitable for solid-state hydrogen storage in pristine state, because of inappropriate thermal dehydrogenation properties (Figure 1). This is due to the occurrence of melting and subsequent foaming, dehydrogenation mainly taking place from about 100 °C, high extent decomposition with release of unwanted by-products over the temperature range 100-200 °C, and formation of polymeric residues of complex composition [81-83].

As a consequence, alkali amidoboranes MAB (with M = Li, Na, K, Rb, Cs) and alkali hydrazinidoboranes MHB emerged (Figure 2).

3.2. Syntheses

Substitution of $H^{\delta+}$ of NH_3 or N_2H_4 by M^+ is relatively easy. In HB, the substituted $H^{\delta+}$ is one on the central N, and the terminal NH_2 moiety remains undisturbed, giving then the formula $NH_2NH(M)BH_3$; the middle N retains a tetrahedral sp^3 hybridization. Two main routes, as discussed hereafter, were developed for the syntheses of MAB and MHB (Tables 1 and 2) [27,84-102].

Syntheses of MAB and MHB must be performed under inert atmosphere (He, Ar or N_2). The reactants (MH or M) as well as the products (MAB and MHB) are not stable under air, especially when air is humid (occurrence of spontaneous hydrolysis). For instance, NaAB evolves under air (mass increase of 48.7%) towards the formation of e.g. sodium carbonate Na_2CO_3 [90] and generates H_2 by solvolysis when put into contact with water or methanol [92]. Two other examples are RbAB and CsAB. They decompose in air within minutes [94] and are moisture sensitive [95].

The light MAB or MHB compounds, i.e. with M as Li and Na, are usually prepared by mechano-chemistry, milling AB or HB with the alkali hydride MH:

$$MH + NH_3BH_3 \rightarrow MNH_2BH_3 + H_2 \quad (8)$$

$$MH + N_2H_4BH_3 \rightarrow MN_2H_3BH_3 + H_2 \quad (9)$$

Generally, MAB and MHB are synthesized in mild milling conditions (200 rpm) in order to avoid unwanted decomposition induced by mechanical heating of the powder. For LiAB and LiHB, extensive milling time (< 1h) induces phase transition into metastable polymorphs [84,97]. With respect to NaAB, the milling conditions are softer because NaH is more reactive than LiH [103]. Mixing equimolar amounts of NaH and NH_3BH_3 with a spatula in a mortar under argon atmosphere for 15 min is for example enough to get pure NaAB [92]. The trend is similar for LiHB and NaHB, because LiH is relatively inert towards HB (enthalpy of reaction <0.1 kJ mol^{-1}) [104], LiHB is formed by ball milling only [96-99]. With respect to NaHB, it has to be synthesized at −30 °C [100], otherwise the reactivity is too high leading to its decomposition (enthalpy of reaction −27.8 kJ mol^{-1}) [98,104]. Another approach is to make large AB particles react with small NaH particles in order to restrict the reaction to the interface of these particles and better control the reaction system [105].

LiAB [87], NaAB [87,91] and NaHB [98] may also be prepared by wet chemistry in aprotic solvent, using THF as anhydrous solvent. As for milling, LiH and NaH are mainly used as sources of M^+. Alternatively, $LiNH_2$, $NaNH_2$ and Li_3N can be used [86-88]:

$$MNH_2 + NH_3BH_3 \rightarrow MNH_2BH_3 + NH_3 \quad (10)$$

$$Li_3N + 3NH_3BH_3 \rightarrow 3LiNH_2BH_3 + NH_3 \quad (11)$$

The reaction of $NaNH_2$ and NH_3BH_3 in THF is however less efficient than the process involving NaH, because of slower kinetics (20 h at 25 °C vs 10 min at −3 °C) [91].

Wet chemistry in aprotic solvent is the privileged method for the heavy MAB and MHB compounds (M = K, Rb, Cs). Both KAB (Eq. 8) and KHB (Eq. 9) can be prepared from KH in anhydrous THF [93,98]. For KHB, the use of an autoclave is recommended for safety issues. Solid-solid mixtures have to be avoided because of high reactivity of KH with the borane (shock-sensitive mixture leading to explosive reaction) [98]. In comparison to e.g. NaH, KH has a stronger basicity [103]. In fact, the enthalpy of reaction was found to be −70.3 kJ mol^{-1} for the

solid-solid reaction between KH and HB at 25 °C (under argon); the enthalpy is thrice that of the reaction between NaH and HB [104]. With respect to the Rb and Cs compounds, syntheses are done using metallic alkali elements in anhydrous THF, because RbH and CsH are not commercially available and the reactivity of Rb and Cs are lower which is better from a safety point of view [94,95,101,102]:

$$M + NH_3BH_3 \rightarrow MNH_2BH_3 + 1/2H_2 \quad (12)$$

$$M + N_2H_4BH_3 \rightarrow MN_2H_3BH_3 + 1/2H_2 \quad (13)$$

As these amidoborane and hydrazinidoborane compounds are not soluble in THF, they can be isolated by filtration.

Table 1. Syntheses of MAB with M = Li, Na, K, Rb and Cs. Details about the nature of the source of M^+ (Prec.), molar ratio AB:M^+, synthesis method, milling/stirring conditions, temperature of reaction (Temp.), and atmosphere (Atm.; when available) are given.

Prec.	AB:M^+	Method	Conditions	Temp.	Atm.	Ref.
LiH	1:1	Ball milling	250 rpm / 3 h / Graphite	Room	Ar	[27,84]
LiH	1:1	Ball milling	250 rpm / 1 h	Room	He	[85]
LiH	1:1	Disc milling	3 min milling + 5 min break [a]	Room	Ar	[86]
LiH	1:1.5	Wet chemistry [b]	THF / Stirring 75 min	Room		[87]
$LiNH_2$	1:1	Disc milling	3 min milling + 5 min break [a]	Room	Ar	[86]
Li_3N	4.2:1	Wet chemistry [b]	THF / Stirring 60 min	30 °C	Ar	[88]
NaH	1:1	Ball milling	250 rpm / 3 h / Graphite	Room	Ar	[27]
NaH	1:1	Ball milling	1 h	Room	H_2 (10 bar)	[89]
NaH	1:1	Disc milling	3 min milling + 5 min break [a]	Room	Ar	[86]
NaH	1:1	Disc milling		Room		[90]
NaH	1:1.2	Wet chemistry [b]	THF / Stirring 10 min	Room		[87]
NaH	1:1	Wet chemistry [b]	THF / Stirring 10 min	−3 °C		[91]
NaH	1:1	Simple mixing	15 min	Room	Ar	[92]
$NaNH_2$	1:1	Wet chemistry [b]	THF / Stirring 20 min	25 °C		[87]
KH	1:1	Wet chemistry [b]	THF / 4 h	Room	N_2/Ar	[93]
KH	1:1	Wet chemistry [b]	Benzene / 48 h	Room	N_2/Ar	[93]
Rb	1:0.93	Wet chemistry [b]	THF / Overnight	0 °C	Ar	[94]
Rb	1:1	Wet chemistry [b]	THF / 24 h	Room	Ar	[95]
Cs	1:1.03	Wet chemistry [b]	THF / Overnight	0 °C	Ar	[94]
Cs	1:1	Wet chemistry [b]	THF	Room	Ar	[95]

[a] The number of cycles has not been mentioned
[b] In aprotic solvent

3.3. Crystalline solids

Like AB and HB [96,106], MAB and MHB are crystalline (Table 3). The lightest MAB has two allotropes: α-LiAB and β-LiAB [27,84,85]. During the mechano-synthesis, the α phase forms first, and transforms to the β phase as the milling progresses [84]. The reverse transition, β-LiAB $\rightarrow$ α-LiAB, takes place upon extended ball milling or by recrystallization after the dissolution of the β phase. Both polymorphs crystallize in the orthorhombic space group *Pbca*. The unit cell of the β phase is twice that of the α phase (with Z = 16 and 8, and for comparable volumes per formula unit such as 67.7 and 63.7 $Å^3$ respectively). The crystal structure of β-LiAB consists of 2D layers of LiAB molecules stacked along the *a* axis. This phase has a lower symmetry than the α phase, and it is seen as a metastable phase arising from energetic milling. Four $[NH_2BH_3]^-$ anions surround each Li^+ cation (Figure 3), via one Li–N bond and three Li···H–BH_2 interactions. The tetrahedral coordination is more distorted for β-LiAB than for α-LiAB.

Table 2. Syntheses of MHB with M = Li, Na, K, Rb and Cs. Details about the nature of the source of M^+ (Prec.), molar ratio HB:M^+, synthesis method, milling/stirring conditions, temperature of reaction (Temp.), atmosphere (Atm.) are given.

Prec.	HB:M^+	Method	Conditions	Temp.	Atm.	Ref.
LiH	1:1	Ball milling	200 rpm / 1-3 h	Room	He (1 bar)	[96]
LiH	1:1	Ball milling	200 rpm / 10 min + 20 min [a]	Room	Ar	[97]
LiH	1:1	Ball milling	150 rpm / 16 h [b]	Room	He	[98]
LiH	1:1	Ball milling	300 rpm / 6 h	Room	Ar	[99]
NaH	1:1	Wet chemistry [c]	THF / 300 rpm	0 °C	Ar	[98]
NaH	1:1	Ball milling	250 rpm / 10 min	−30 °C	Ar	[100]
KH	1:1	Wet chemistry [c]	THF / 300 rpm	25 °C	Ar	[98]
Rb	1.15:1	Wet chemistry [c]	THF / 30 h	Room	Ar	[101]
Cs	1.15:1	Wet chemistry [c]	THF / 6 h	Room	Ar	[102]

[a] 10 min milling followed by 20 min break, 18 times
[b] 1 min milling in one direction + 15 s break + 1 min in the other direction, for 16 h
[c] In aprotic solvent

LiHB also has two polymorphs, crystallizing, however, in different space groups. Interestingly, as for LiAB, the metastable phase, which was originally discovered (hereafter denoted α-LiHB), can be stabilized at ambient conditions through energetic ball milling. However, contrary to LiAB, the stable phase, published later, named β-LiHB (orthorhombic, s.g. *Pbca*), transforms into α-LiHB (monoclinic, s.g. $P2_1/c$) upon heating [96-100,107]. The phase transition β-LiHB $\rightarrow$ α-LiHB occurs when the β phase is heated at 95 °C for 2 h or at 90-91 °C while heated at 5 °C min^{-1} from room temperature. For each phase, the Li^+ cation has a tetrahedral environment

(Figure 4), interacting with four $[N_2H_3BH_3]^-$ anions. There is a first Li–N bond $NH_2NH(Li)BH_3$, a second Li–N bond with the lone electron pair of the terminal N atom of another anion, and two Li···H_2–BH interactions. The better stability of *β*-LiHB can be rationalized by a longer distance between two Li^+ cations (3.49 Å vs 3.31 Å for *α*-LiHB), higher density (1.061 vs 1.047 for *α*-LiHB) and a more distorted tetrahedral environment.

Table 3. Summary of crystallographic properties of MAB and MHB compounds (Comp.) with M = Li, Na, K, Rb and Cs. Information that is provided is as follows: unit cell, space group (s.g.), cell parameters (*a*, *b*, *c*, □; for the clarity of the comparison, the parameters are given with three digits), and number of formula unit per unit cell (Z).

Comp.	**Unit cell** [a]	**s.g.**	***a*** **(Å)**	***b*** **(Å)**	***c*** **(Å)**	***β*** **(°)**	**Z**	**Ref.**
AB	Tetrag.	*I4mm*	5.263	5.263	5.050	90	2	[106]
α-LiAB	Orthor.	*Pbca*	7.113	13.949	5.150	90	8	[27]
α-LiAB	Orthor.	*Pbca*	7.105	13.930	5.148	90	8	[85]
β-LiAB	Orthor.	*Pbca*	15.146	7.721	9.268	90	16	[84]
NaAB	Orthor.	*Pbca*	7.469	14.655	5.653	90	8	[27]
NaAB	Orthor.	*Pbca*	7.464	14.635	5.648	90	8	[91]
NaAB	Orthor.	*Pbca*	7.474	14.645	5.674	90	8	[91]
KAB	Orthor.	*Pbca*	9.430	8.261	17.340	90	16	[93]
α-RbAB	Monocl.	$P2_1/c$	6.931	5.015	11.074	101.688	4	[95]
β-RbAB	Cubic	$Fm\underline{3}m$	7.328	7.328	7.328	90	4	[95]
α-CsAB	Orthor.	*Pnam*	9.119	7.345	5.969	90	4	[95]
β-CsAB	Cubic	$Fm\underline{3}m$	7.596	7.596	7.596	90	4	[95]
HB	Orthor.	*Pbcn*	13.123	5.100	9.581	90	8	[96]
α-LiHB	Monocl.	$P2_1/c$	5.852	7.466	8.897	122.381	4	[96]
β-LiHB	Orthor.	*Pbca*	10.252	8.479	7.469	90	8	[97]
NaHB	Monocl.	$P2_1/n$	4.974	7.958	9.292	93.814	4	[100]
KHB	Monocl.	$P2_1$	6.709	5.882	5.767	108.268	2	[98]
RbHB	Monocl.	$P2_1$	5.813	6.701	5.814	108.915	2	[101]
CsHB	Monocl.	$P2_1$	5.916	7.009	6.002	108.389	2	[102]

[a] Tetrag. for tetragonal; Orthor. for orthorhombic; Monocl. for monoclinic.

NaAB and KAB are isostructural to LiAB [27,91,93]. Like for Li^+, Na^+ has a tetrahedral coordination via one Na–N bond and three Na···H_2–BH interactions (Figure 3). The K^+ cation is larger and can accommodate more ligands. It is octahedrally coordinated (Figure 3), with six $[NH_2BH_3]^-$ anions, i.e. in *mer* symmetry involving two K–N bonds, two K···H–BH_2 and two K···H_2–BH interactions.

Unlike the aforementioned amidoboranes, β-LiHB, NaHB and KHB crystallize in different monoclinic cells (*Pbca*, $P2_1/n$, $P2_1$ respectively) [96,98,100]. For NaHB, there is one more anion

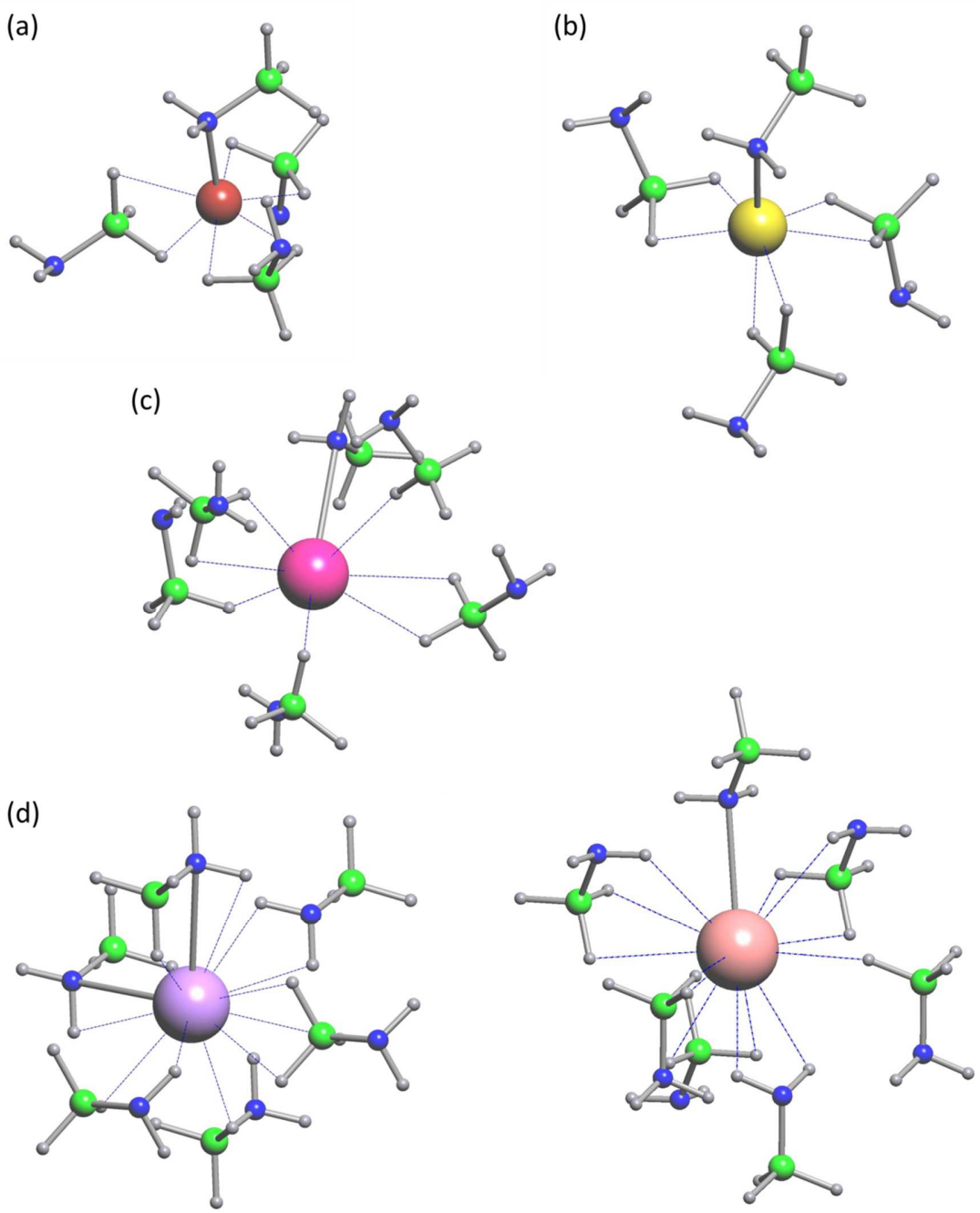

Figure 3. Cation environment of: (a) LiAB, (b) NaAB, (c) KAB, (d) RbAB, (e) CsAB. The green, blue and grey spheres represent the B, N and H atoms respectively. The other colored spheres show the alkali elements.

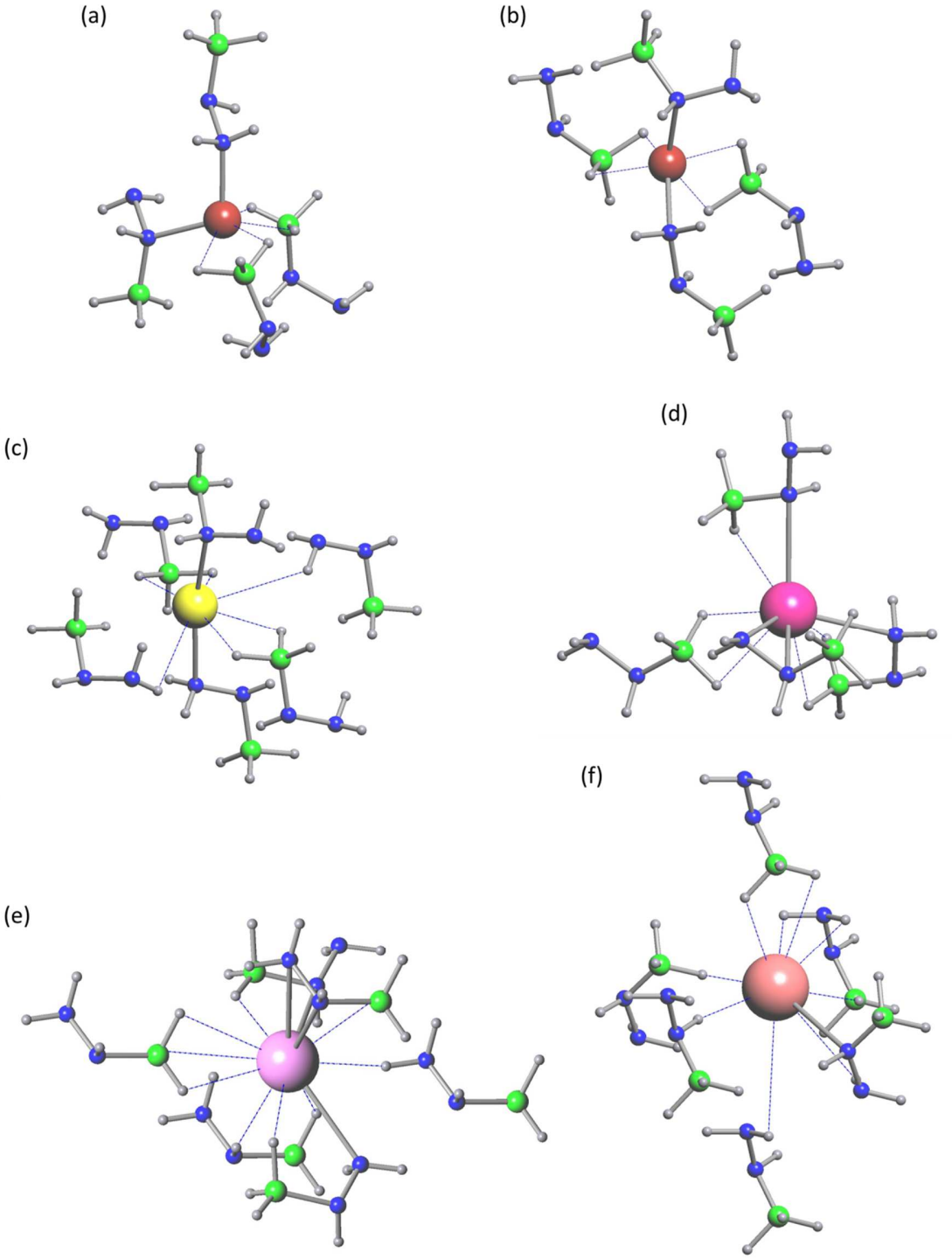

Figure 4. Cation environment of: (a) α-LiHB, (b) β-LiHB, (c) NaHB, (d) KHB, (e) RbHB, (f) CsHB. The green, blue and grey spheres represent the B, N and H atoms respectively. The other colored spheres show the alkali elements.

around the cation; five $[N_2H_3BH_3]^-$ anions surround Na^+, suggesting trigonal bipyramidal geometry (Figure 4). As for LiHB, there are two Li–N bonds, one with the central N and one with the terminal N, at the apical positions. At the equatorial positions, the coordination is made through two Na···H_2–BH and one Na···H–BH_2 interactions. As for K^+ in KHB, the number of surrounding anions is four (Figure 4). It interacts more intimately with the surrounding anions than Na^+ does. One of the $[N_2H_3BH_3]^-$ anions is coordinating K^+ through both of its N, one K–N bonds with internal N atoms, and another with the lone pair of electrons on the terminal N. Among the three remaining coordinating anions; one is forming the K–N bond with the central N and the other two are forming K···H_2–BH interactions.

The amidoboranes of heavier alkali elements, i.e. RbAB and CsAB [94,95], do not share the *Pbca* symmetry of LiAB, NaAB, and KAB. RbAB crystallizes in a monoclinic system (space group $P2_1/c$) where each Rb^+ cation coordinates six $[NH_2BH_3]^-$ anions according to a pseudo-octahedron (Figure 3). On the other hand, each $[NH_2BH_3]^-$ anion has a distorted octahedral environment, being surrounded by six Rb^+ cations. With respect to CsAB, it has a primitive orthorhombic structure, the space group being *Pnam*. Seven $[NH_2BH_3]^-$ anions surround each Cs^+ (Figure 3). Both amidoboranes, denoted α-RbAB and α-CsAB, undergo, upon heating, a reversible phase transition. At 50 and 60°C form respectively β-RbAB and β-CsAB. Both of these β phases have a cubic $Fm\underline{3}m$ unit cell.

As for KHB, RbHB and CsHB crystallize in a monoclinic $P2_1$ space group [101,102]. The cations Rb^+ and Cs^+ have an octahedral coordination, with six surrounding $[N_2H_3BH_3]^-$ anions (Figure 4).

With MAB [27,93,95], the volume of the unit cell per formula unit increases with the size of the metal cation (Figure 5). It has a pseudo-linear evolution consistently with the increase of the ionic radius of M^+ from Li^+ to Cs^+. However, the situation is different with MHB [96,98,100-102]. Unlike stated elsewhere [108], the volume of the unit cell per formula unit does not follow a constant evolution (Figure 5): it decreases from LiHB to NaHB, increases from NaHB to KHB, decreases from KHB to RbHB, and increases from RbHB to CsHB. Two factors may explain this. The first one may be the non-linear evolution of the number of coordinating $[N_2H_3BH_3]^-$

anions, since it is 4 for Li^+, it increases to 5 for Na^+, it decreases to 4 for K^+, and it increases to 6 for Rb^+ and Cs^+. The second one may be related to the presence of two N atoms (versus one for MAB) which may enhance the number of interactions resulting in compacter cation environments.

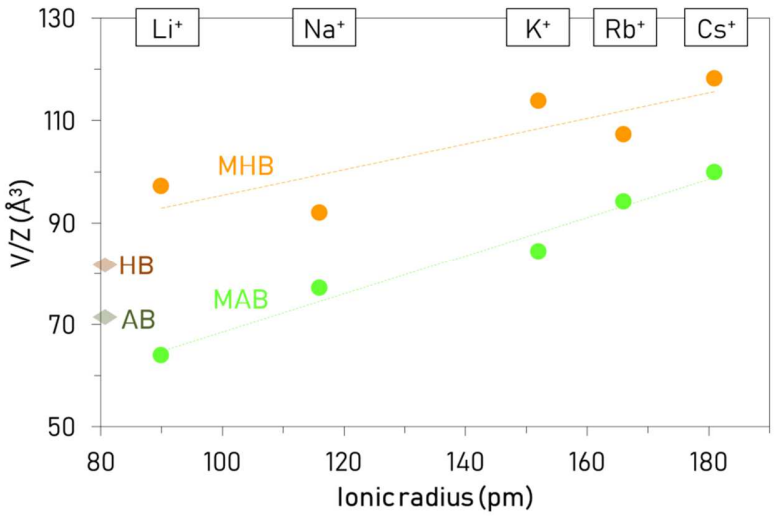

Figure 5. Evolution of the cell volume normalized by the number of formula unit per unit cell (V/Z in $Å^3$) as a function of the ionic radius of the alkali cations (Li^+, Na^+, K^+, Rb^+, Cs^+), for MAB and MHB. The V/Z value for both AB and HB are indicated by diamonds on the *y* axis.

3.4. Ionic salts and Lewis bases

Substitution of $H^{\delta+}$ in AB or in HB by M^+ (Figure 6) results in M–N bonds with ionic character [109]. Another consequence of the substitution of $H^{\delta+}$ by M^+ is a change of the length of the B–N bond (Figure 7) [27,93,95,96,98,100-102]. It is slightly shorter for MAB and MHB in comparison to the bond in AB and HB. For example, in α-LiAB, NaAB and α-RbAB, the bond lengths are 1.56, 1.53, and 1.54 Å respectively, whereas it is 1.6 Å for AB. Regarding hydrazinidoboranes, for both LiHB and RbHB, the bond length is 1.55 Å and, for both NaHB and KHB, it is 1.54 Å, versus 1.59 Å for HB. It is worth mentioning that the B–N bond shortening in MAB and MHB is featured by a downfield shift of the ^{11}B resonance (Figure 8) [89,94,98,101], which evidences a strong electronic rearrangement in the $[NH_2BH_3]^-$ and $[N_2H_3BH_3]^-$ entities [110]. More electronic density is attracted by N from M^+ than from $H^{\delta+}$, the Lewis basicity of the N-containing group is reinforced, the B–N bond becomes stronger, the ionic character of $H^{\delta-}$ on

B is increased, and as consequence, $H^{\delta-}$ is a stronger Lewis base (i.e. more reactive than in AB or HB) [27,45,85,98].

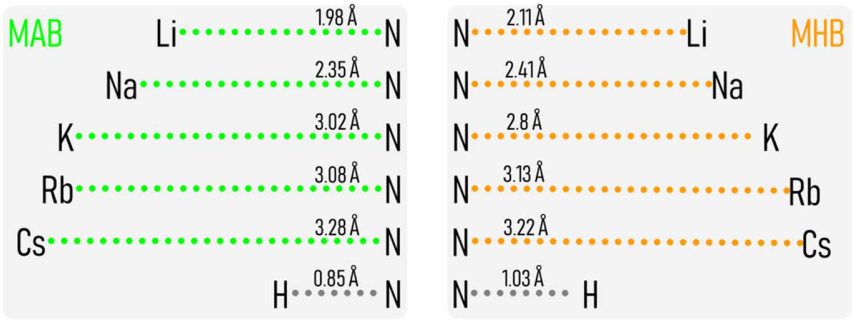

Figure 6. Evolution of the M–N bond lengths of MAB and MHB. The H–N bonds lengths for both AB and HB are also indicated.

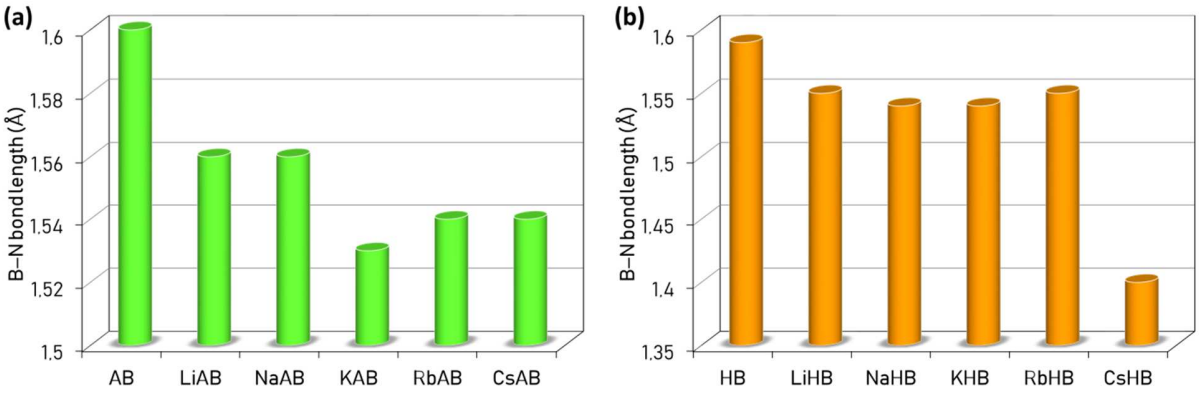

Figure 7. Evolution of the B–N bond lengths of MAB and MHB (except for CsHB for which it has not been determined yet). The bonds lengths for both AB and HB are also indicated.

For MHB, the N–N bond is negligibly impacted by M^+ that may also interact with the lone electron pair of the terminal N of the $[N_2H_3BH_3]^-$ anion, as discussed in the previous section. The N–N bond distance is comparable for HB (1.46 Å) [96], *α*-LiHB (1.47 Å) [96], NaHB (1.46 Å) [100], and KHB (1.46 Å) [98]. There are exceptions. With *β*-LiHB, the N–N bond (1.50 Å) is slightly longer [97]. RbHB has a slightly shorter bond (1.43 Å) [101] and, for CsHB, the bond is much shorter at 1.30 Å [102].

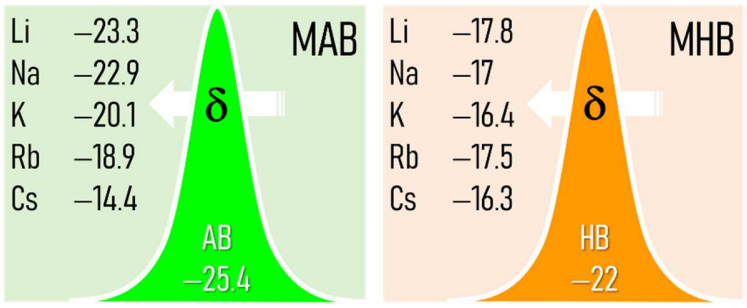

Figure 8. Illustration of the downfield shift of the ^{11}B signal (from magic angle spinning nuclear magnetic resonance spectrum; δ in ppm) from AB to MAB and from HB to MHB.

3.5. Dihydrogen bonding

One of the peculiarities of fundamental interest with B-N-H compounds is the existence of an intermolecular dihydrogen network owing to $H^{\delta+}\cdots H^{\delta-}$ interactions. The intermolecular $H^{\delta+}\cdots H^{\delta-}$ distance is 2.02 Å in AB [111] and 2.01 Å in HB [79]. These distances are shorter than the sum of the van der Waals radii for two H atoms (2.4 Å), due to dihydrogen $H^{\delta+}\cdots H^{\delta-}$ bonding.

Weakened intermolecular dihydrogen bonding characterizes MAB and MHB [93]. The $H^{\delta+}\cdots H^{\delta-}$ distances are longer than those determined for AB or HB, but they remain less than the van der Waals distance, confirming weaker dihydrogen interactions [95]. For instance, the $H^{\delta+}\cdots H^{\delta-}$ distance is 2.25 Å in the case of α-LiAB and of β-LiHB [85,98]. Dihydrogen $H^{\delta+}\cdots H^{\delta-}$ interactions are also present within each $[NH_2BH_3]^-$ or $[N_2H_3BH_3]^-$ anion. They have distances of 2.00-2.10 Å in $[N_2H_3BH_3]^-$ of α-LiHB for example [96].

Head-to-tail $H^{\delta+}\cdots H^{\delta-}$ interactions take part in the stabilization of the solid state. In fact, not only these interactions play a role. Homopolar $H^{\delta+}\cdots H^{\delta+}$ and $H^{\delta-}\cdots H^{\delta-}$ interactions also contribute to the stability of MAB and MHB [112]. However, the van der Waals interactions between M^+ and the anionic entities predominate: they supersede the dihydrogen bonding and are of sufficient energy so that MAB and MHB are crystalline solid at ambient conditions [87,93]. Elsewhere, for LiAB, Najiba and Chen stressed on the absence of dihydrogen bonding and on the key role of the van der Waals interaction between Li^+ and $H^{\delta-}–BH_2$ [113].

3.6. Thermal dehydrogenation

Compared to AB and HB, all of the MAB and MHB compounds have shown better dehydrogenation properties with lower temperatures of dehydrogenation and higher purity of the released H_2.

LiAB dehydrogenates at temperatures below 100 °C following a near thermally neutral event (−3 kJ mol^{-1}) [27,84], knowing that the α phase of LiAB is more supportive for H_2 release [114]. NaAB has slightly better dehydrogenation properties. For example, heated at ca. 80°C, NaAB requires 92 s to liberate 0.5 equiv H_2 versus 3017 s for LiAB [87]. For both materials, the purity of the released H_2 is controversial. On one side, H_2 was reported to be pure [27,85,87,91]; on the other side, H_2 was found to be polluted by NH_3 [86,90,115]. KAB has also attractive dehydrogenation properties [93], but the results cannot be compared to those of LiAB and NaAB because of the discrepancies in the experimental conditions and devices. KAB liberates 1.5 equiv H_2 up to ca. 100 °C, without any pollutant [93]. Both RbAB and CsAB decompose from ca. 65 and 55 °C respectively and below 100 °C, releasing H_2 and significant amounts of NH_3 [94,95]. According to theoretical calculations made on the molecular level, the least stable MAB would be LiAB and the most stable would be CsAB, such as LiAB < NaAB < KAB < RbAB < CsAB [116,117]. This is in contradiction with the experimental observations made on the material level (i.e. $\geq 10^{20}$ molecules) which suggest a reverse ranking. CsAB is the least stable, knowing that Cs has the lower electronegativity; the stability of MAB would be driven by the metal electronegativity [77].

The high-temperature phase α-LiHB is responsible for a two-step decomposition occurring above 90 °C [96,97,107]. Together with H_2, N_2 is released, but also some NH_3. The dehydrogenation properties of NaHB are more attractive [98,100]. It releases H_2 from ca. 60 °C and a total of ca. 2 equiv H_2 up to 100°C. The decomposition mechanism is, however, a bit complex as it is composed of three successive dehydrogenation processes and one denitrogenation process. Some N_2 and traces of N_2H_4 and NH_3 contaminate the H_2 stream. In contrast, when NaHB is “doped” with a slight excess of NaH, pure H_2 is generated [118]. With KHB, dehydrogenation takes place at lower temperatures, from ca. 50 °C [98]. Small amounts of NH_3 and N_2 are also generated. RbHB decomposes from ca. 60 °C and releases 5 wt. % of H_2 and NH_3 within the temperature

range 60-100 °C [101]. With regard to CsHB, it decomposes from ca. 75°C and up to 160 °C the weight loss is 3.5 wt. % because of the release of NH_3 together with H_2. Two additional weight losses occur between 160 and 250 °C, resulting in the release of 6.9 wt. % of gases; NH_3 is thus the main gaseous product with CsHB [102]. Though CsHB seems to be slightly more stable than RbHB, there is a rough correlation between the MHB reactivity and the alkali element electronegativity: the lower the electronegativity is, the less stable the MHB is [77].

Exact identification of the thermolysis solid residue recovered upon dehydrogenation of MAB and MHB is challenging. An amorphous (or poorly crystalline) residue systematically forms, which renders powder X-ray diffraction of little assistance. The technique however allows seeing the formation, over 200 °C, of crystalline by-products such as NaH, RbH, and CsH [90,91,95].

During its thermal decomposition, NaAB is supposed to transform into: a small amount of NaH (as detected by ^{23}Na NMR spectroscopy) [89,90], and mainly into an amorphous solid being either a mixture of boron nitride and polyiminoborane-like structures [89] or boron nitride [91] (Figure 9). The formation of polyaminoborane as a transient phase is discarded. In general, the thermolysis residue forming from MAB is considered as being polyborazylene- and polyiminoborane-like compounds [27,84-93,115].

With respect to MHB, the nature of the thermolysis residue is as complex. Polymeric compounds having tetragonal boron environments (i.e. $\mathit{B}H_4$, $N\mathit{B}H_3$, $N_2\mathit{B}H_2$) as well as trigonal boron environments (i.e. $N\mathit{B}H_2$, $N_2\mathit{B}H$, BN_3) form [97-102]. These environments are systematically discussed as polymeric B–N-based compounds (Figure 9).

Because the thermolysis residues coming from MAB and MHB have not been well identified yet, the dehydrogenation mechanisms are also not well known. However, there are some elements, which may help in better understanding the dehydrogenation mechanisms of MAB and MHB.

With pristine AB, before any H_2 release, the compound dimerizes into diammoniate of diborane $[(NH_3)_2BH_2]^+[BH_4]^-$ [119]. A comparable intermediate was predicted for LiAB [120]: $[LiNH_2BH_2LiNH_2]^+[BH_4]^-$, considered also as a Li–H–Li complex. It would allow thermoneutral

H_2 release via formation of a coiled polymeric product such as $LiNH_2BH_2LiNHBH_3$. Another predicted species is the dianion $[NHBHNHBH_3]^{2-}$ [121].

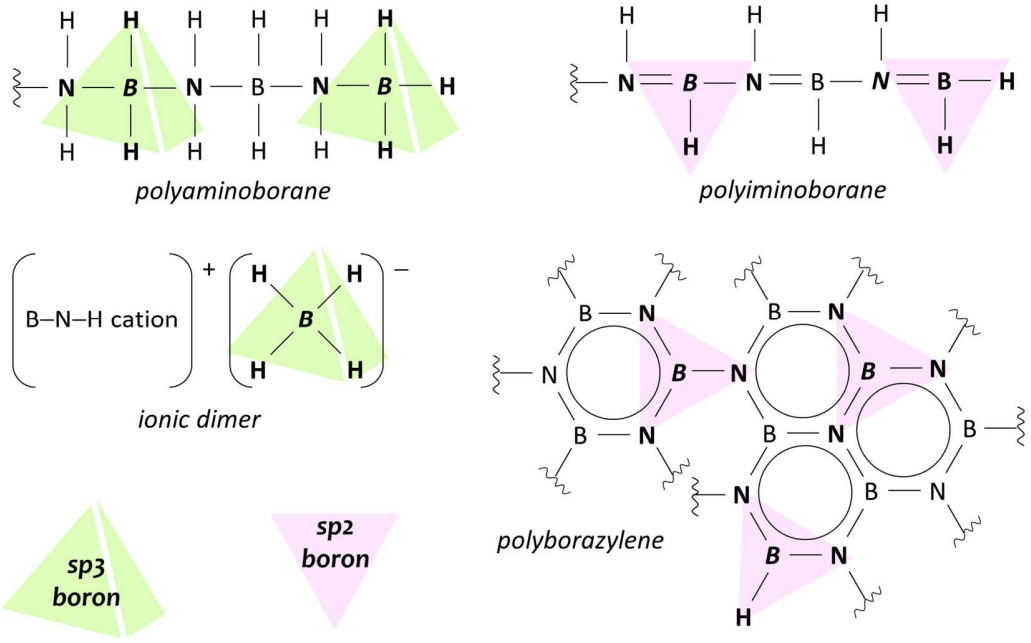

Figure 9. Examples of compounds having tetragonal boron environments (i.e. BH_4, NBH_3, N_2BH_2) and trigonal boron environments (i.e. NBH_2, N_2BH, BN_3).

For NaAB, the formation of an ionic dimer resembling those mentioned above was, on one hand, discarded because ^{11}B NMR analyses did not show signals belonging to N_2BH_2 and BH_4 environments [89]. On the other hand, a head-to-tail dimerization into the ionic salt $[NH_3Na]^+[BH_3(NHNa)BH_3]^-$ was proposed because it would explain the release of NH_3 at >55 °C and the formation of NaH (Figure 10). The as-formed $BH_3(NHNa)BH_2$ liberates H_2 above 55 °C. This is a minor mechanism, estimated to have a contribution of 10%. The major mechanism is based on intramolecular dehydrogenation of NaAB.

The most frequently discussed mechanism is different. It is based on the key role of the in situ forming metal hydride M–H. In an initial step, it is believed to form by $H^{\delta-}$ transfer from e.g. $[NH_2BH_3]^-$ to M^+. The mechanism is called metal ion assisted hydride transfer or metal cation

driven hydride-transfer. It takes place involving one MAB compound [122-126]; the M–H formed induces low temperature dehydrogenation such as:

$$MNH_2BH_3 \rightarrow MH\cdots H{-}NHBH_2 \rightarrow MNHBH_2 + H_2 \quad (14)$$

A comparable mechanism involves two MAB compounds (Figure 11) [87], which follows the formation of intermolecular N–B bonds (towards oligomeric/polymeric residues). Note that, instead of LiH, Li_3–H would be a possible intermediate phase for trimeric and tetrameric clusters of LiAB [127,128], and Li_2–H an intermediate phase for dimeric LiHB [129]. The metal ion assisted hydride transfer is consistent with the relationship made between the reactivity of MAB (or MHB) and the electronegativity of M: more active alkaline elements (i.e. those having lower electronegativity) are more likely to favor H transfer via the formation of M–H [77].

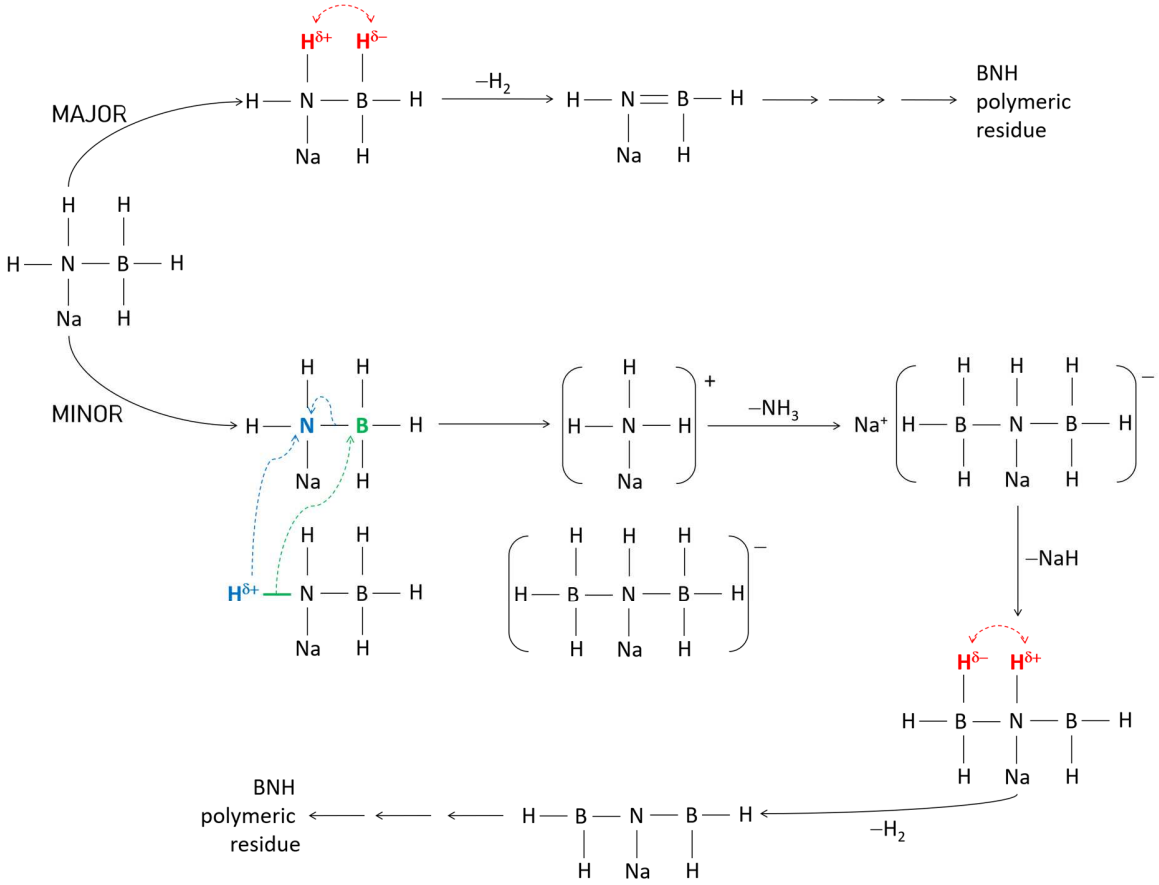

Figure 10. Mechanisms (major and minor, such as 90 and 10% respectively) of thermal dehydrogenation proposed for MAB. Adapted from ref. [84,88].

Another intermediate to mention is $[NH_3M]^+[BH_3NH_2BH_2NH_2BH_3]^-$, forming from three MAB compounds. This "trimeric" intermediate was presented as the missing link in the mechanisms of MAB dehydrocoupling, and results in the formation of $[M]^+[BH_3NH_2BH_2NH_2BH_3]^-$, plus NH_3 that evolves [130].

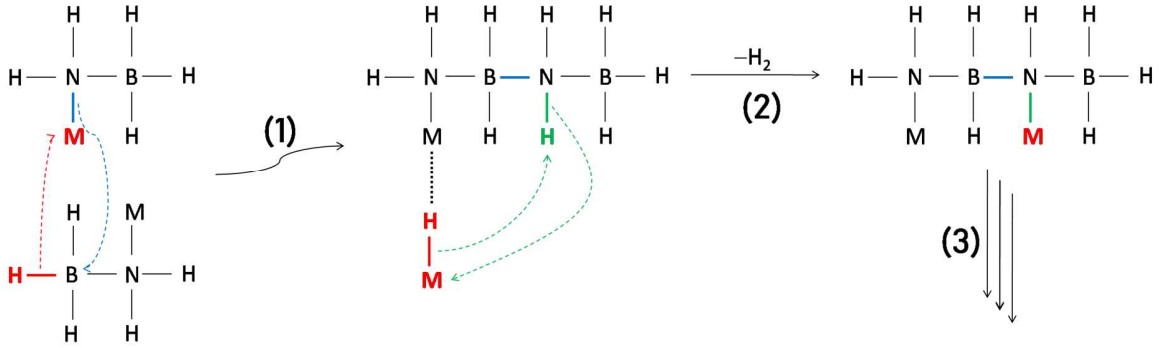

Figure 11. Illustration of the metal ion assisted hydride transfer involving two MAB molecules: (1) formation of M–H by intermolecular reaction (dimer formation) followed by stabilization via an $M–H^{\delta-}\cdots M^+–N$ interaction; (2) dehydrogenation by reaction of M–H with H–N; (3) successive dehydrocoupling of dimers formed. Adapted from ref. [87].

With respect to dehydrogenation of MHB, it is likely that diammoniate of diborane-like species are involved as transient phases. Suggested examples are as follows: $[(LiN_2H_3)_2BH_2]^+[BH_4]^-$ [97] and $[(NaN_2H_3)_2BH_2]^+[BH_4]^-$ [100]. Other examples are non-ionic dimers, like $NH_2NH(M)BH_2NHNH(M)BH_3$ and $NH_2NH(M)BHNNH(M)BH_3$ (M = Li, Na, K) [98]. According to computational calculations, dimers of NaHB may play the major role in the dehydrogenation pathway [131].

Intuitively, it was long believed that dehydrogenation of B–(N–)H compounds occurs via heteropolar $H^{\delta+}\cdots H^{\delta-}$ reactions only. However, dehydrogenation also implies counterintuitive homopolar $H^{\delta-}\cdots H^{\delta-}$ and $H^{\delta+}\cdots H^{\delta+}$ reactions [24,132-134]. For example, when heated, $LiND_2BH_3$ releases a significant quantity of H_2 along with HD, and the existence of homopolar $H^{\delta-}\cdots H^{\delta-}$ reactions explains the formation of H_2 [112]. When heated, $LiN_2H_3BD_3$ generates appreciable amounts of HD, H_2 and D_2, and the formation of all of these gases is explained by the existence of a multitude of H(D) ···H(D) interactions [99]. Initial thermal dehydrocoupling takes place

through homopolar $H^{\delta+}\cdots H^{\delta+}$ interactions at low temperature. This step is followed by heteropolar $H^{\delta+}\cdots D^{\delta-}$ and homopolar $D^{\delta-}\cdots D^{\delta-}$ pathways.

3.7. Closing the hydrogen cycle

The dehydrogenation of MAB and MHB is exothermic, and the rehydrogenation of the thermolysis residue under H_2 pressure is thermodynamically unfavorable. A few unsuccessful attempts were published. A first one was performed on $LiBNH_{1.32}$ (a by-product of LiAB heated up to 200 °C) at 50 bar of H_2 up to 250 °C, no hydrogenation was recorded [85]. A second one was done on $[BN]_n$ (a by-product of NaAB) at 120 bar H_2 and was ineffective [91].

Alternatively, MAB can be regenerated by chemical recycling/reduction of its residue. There is one effective regeneration path that has been successfully applied to polyborazylene that is generally taken as a model residue of AB. Polyborazylene can be recycled back into AB by reduction using N_2H_4 in NH_3 medium [135]. The same path was applied to a residue of LiAB identified as being made of cross-linked polyborazylene-based structures (Figure 12) [136]. The conversion back to LiAB was found to be 63%. To explain this value lower than 100%, it was conjectured that part of the regenerated LiAB decomposed during the hydrogenation process. In our opinion, there may be another reason. The aforementioned reduction process is efficient on polyborazylene only, whereas residues from MABs (and MHBs) are of complex composition, involving not only polyborazylene-like compounds but also polyiminoborane- and polyiminoborane-like compounds (without considering amorphous and/or hexagonal boron nitride). In any case, the formation of boron nitride must be avoided because it is chemically stable, which then excludes chemical recycling/reduction [137].

There is another regeneration approach [138], which is in fact similar to the recycling approaches developed so far for the borate $NaB(OH)_4$ stemming from $NaBH_4$ hydrolysis (Figure 12) [139]. A residue (denoted MBNH for clarity, with M = Li, K) is first digested by methanol to form $B(OCH_3)_3$, and second, the obtained product is reduced by lithium alanate $LiAlH_4$ in the presence of a source of NH_3 in the form of ammonium chloride NH_4Cl. This regeneration approach results in the formation of AB, which can finally be reacted with MH (e.g. Eq. 8) to regenerate the MAB. The energy efficiency of this stepwise process is actually not attractive (ca. 46%).

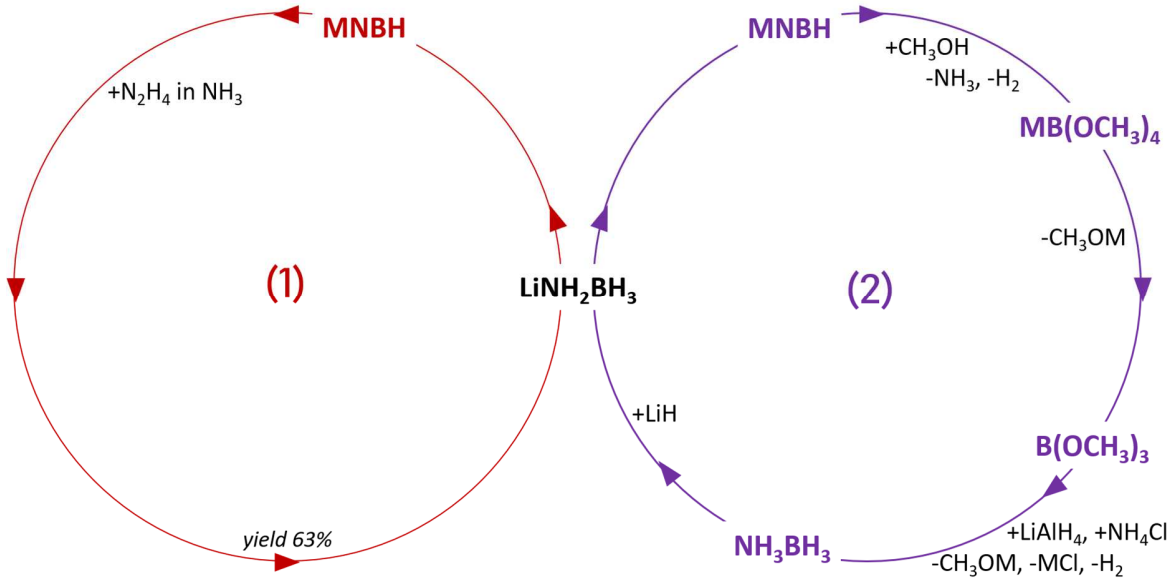

Figure 12. Closing the cycle with LiAB: (1) reduction of the residue MNBH by N_2H_4 in the presence of NH_3 as solvent (yield reported to be 63% in ref. [136]); (2) digestion of MNBH by methanol and reduction of the as-forming $B(OCH_3)_3$ by $LiAlH_4$ in the presence of NH_4Cl to form AB as starting material of LiAB (as reported in ref. [138]).

4. Alkaline earth amidoboranes and hydrazinidoboranes

4.1. Beryllium amidoborane, virtually

Beryllium is highly toxic (and carcinogenic) and has not been considered as a possible cation of AB and HB derivatives. It is however possible to envisage its "use" virtually.

$Be(AB)_2$ and $Be(HB)_2$ would be attractive owing to high gravimetric hydrogen densities (Figure 2). By computational calculations, $Be(AB)_2$ is predicted to have a *C*2 symmetry where each Be^{2+} cation would be tetra-coordinated. The Be–N distance would be 1.647 Å. The B–N bond (1.588 Å) would be shorter than that of AB, and the B–N bond stronger [140,141]. Elsewhere, $Be(AB)_2$ is predicted to have a $P\underline{1}$ symmetry where each Be^{2+} cation would be bi-coordinated [117].

4.2. Magnesium amidoborane and hydrazinidoborane

The first attempts for synthesizing $Mg(AB)_2$ by ball milling MgH_2 (or Mg) with two equivalents of AB failed. Both MgH_2 and Mg were apparently inert against AB [85,142]. A weaker Lewis basicity than that of e.g. LiH, NaH and CaH_2 may explain the apparent inertness of MgH_2. For the synthesis of $Mg(AB)_2$, the key is patience. Under argon atmosphere, the mixtures MgH_2-2AB and Mg-2AB slowly evolve as follows [143]:

$$MgH_2 + 2NH_3BH_3 \rightarrow Mg(NH_2BH_3)_2 + 2H_2 \quad (15)$$

$$Mg + 2NH_3BH_3 \rightarrow Mg(NH_2BH_3)_2 + H_2 \quad (16)$$

At room temperature, the waiting time is between 45 days and 6 months. The process time can be decreased to 60-90 h by increasing the ageing temperature to 40 °C.

The crystal structure of $Mg(AB)_2$ has not been solved yet through X-ray diffraction analysis. A modeled structure was proposed in a monoclinic *C*2 unit cell using Monte Carlo algorithm (Table 4). In this structure, the Mg^{2+} cation is tetra-coordinated to four $[NH_2BH_3]^-$ anions, and the Mg–N bond is ionic [144].

Table 4. Summary of crystallographic properties of $M(AB)_2$ and $M(HB)_2$ compounds (Comp.) with M = Mg, Ca, and Sr. Information that is provided is as follows: unit cell, space group (s.g.), cell parameters (*a*, *b*, *c*, *β*; for clarity, the parameters are given with three digits), and number of formula unit per unit cell (Z).

Comp.	Unit cell [a]	s.g.	*a* (Å)	*b* (Å)	*c* (Å)	*β* (°)	Z	Ref.
AB	Tetrag.	*I4mm*	5.263	5.263	5.050	90	2	[106]
$Mg(AB)_2$ [b]	Monocl.	*C*2	8.577	5.605	5.622	85.848	2	[144]
$Ca(AB)_2$	Monocl.	*C*2	9.100	4.371	6.441	93.19	2	[85,146]
$Sr(AB)_2$	Monocl.	*C*2	8.166	5.097	6.726	94.392	2	[147]
HB	Orthor.	*Pbcn*	13.123	5.100	9.581	90	8	[96]
$Ca(HB)_2$	Monocl.	*Ic*	8.260	10.412	11.937	107.515	4	[147]

[a] Tetrag. for tetragonal; Orthor. for orthorhombic; Monocl. for monoclinic.
[b] Modeled structure obtained using Monte Carlo algorithm.

Thermal dehydrogenation of $Mg(AB)_2$ is complex, with three successive steps peaking at ca. 104, 162 and 223 °C [143]. Up to 300 °C, 4.2 equiv H_2 are desorbed, leaving an amorphous residue mainly composed of polyborazylene-like compounds and a small amount of MgH_2 (or Mg). The residue remains unchanged under 100 bar H_2 at 300 °C. The metal ion assisted transfer is proposed as the key mechanism of dehydrogenation (with M = Mg or Ca) [125]:

$$M(NH_2BH_3)_2 \rightarrow (NH_2BH_3)M{-}H \cdots H{-}NHBH_2 \quad (17)$$

The formation of M_3H (with M as Mg, but also as Ca and Sr) was also predicted [145].

Working on hydrazinidoboranes for some years now, we attempted the synthesis of $Mg(HB)_2$ on several occasions. Ball milling MgH_2 and HB (mol ratio 1:2) was found to be unsuccessful in different milling conditions, namely at 200 to 450 rpm for 1 to 18 cycles with milling times varying from 10 to 30 min. Either unreacted MgH_2 and HB were detected by powder XRD or the recovered solid was amorphous to X-ray (except a few diffraction peaks belonging to MgH_2) [104]. Recently we initiated a new series of experiments that are described in the *supporting information* file. We tested different Mg precursors, namely Mg and MgH_2, as well as di-*n*-butylmagnesium $Mg(C_4H_9)_2$. The first two were ball-milled with two equivalents of HB and, for example, put at 50-90 °C. The third precursor was used in dioxane and the mixture of HB and it was even heated up to 70 °C. With MgH_2, we also tried to apply the procedure (described above) successfully applied to $Mg(AB)_2$. Again, all of our attempts failed. Work is still in progress.

4.3. Calcium amidoborane and hydrazinidoborane

Synthesized in THF (Eq. 5), the Ca derivative of AB is coordinated by two solvent ligands such as $Ca(thf)_2(NH_2BH_3)_2$. This complex (single crystal at −153 °C) has an orthorhombic structure (s.g. *Pnmm*). The cell parameters are as follows: a = 7.910 Å, b = 17.570 Å, c = 4.670 Å, V = 649.0 Å^3, and Z = 2 [38].

Synthesizing a pure phase of $Ca(AB)_2$ is challenging, even by ball milling. Intense milling is required to form mixtures where $Ca(AB)_2$ is the major phase; CaH_2 and AB are the minor phases [85,146]. $Ca(AB)_2$ crystallizes in a monoclinic *C*2 unit cell (Table 4) where the Ca^{2+} cation has an octahedral coordination. The shortest Ca−N distance is 2.47 Å. The B−N distance is 1.546 Å, shorter and stronger than the bond in AB, and the hydrogen atoms on B are stronger Lewis bases with increased ionic character.

Computational calculations predicted a covalent Ca−N bond in $Ca(AB)_2$ and thus a lower thermal stability in comparison to $Mg(AB)_2$ that has an ionic Mg−N bond [143]. Indeed, $Ca(AB)_2$ is less stable as it is able to release H_2 from ca. 80 °C, most of the H_2 being generated at 100 and 140 °C [85,146]. Within the temperature range 80-250 °C, $Ca(AB)_2$ generates ca. 3.8 equiv H_2 and

transforms into an amorphous residue suggested to be $Ca_2B_2N_2H_{2.33}$. Hydrogenation of the residue under 50 bar H_2 at 250 °C was unsuccessful. The metal ion assisted transfer mechanism discussed for the alkali amidoboranes was also predicted as playing an important role in the dehydrogenation of $Ca(AB)_2$ [123,145], where dianions such as $[NHBHNHBH_3]^{2-}$ would form [121].

Like for MgH_2, HB does not react with CaH_2 when they are ball milled (at conditions such as 200-450 rpm for 1-18 cycles and 10-30 min) [104]. The reaction was successfully thermally activated [147]. At ca. 60 °C, temperature at which HB melts, solid-state CaH_2 and liquid-state HB were reacted to form $Ca(HB)_2$. The conversion was not total, as crystalline CaH_2 was found together with crystalline $Ca(HB)_2$ in relative amounts of 29 and 71 wt. %. $Ca(HB)_2$ crystallizes in a monoclinic cell with a space group *Ic* (Table 4). The shortest Ca–N distance in $Ca(HB)_2$ is 2.54 Å, which is slightly longer than the distance in $Ca(AB)_2$ (with 2.47 Å).

Under heating, the $Ca(HB)_2$ phase-rich solid decomposes from ca. 90 °C up to 200 °C releasing 5.3 wt. % of gases mainly composed of H_2 with traces of N_2, NH_3 and N_2H_4. In fact, the dehydrogenation extent of $Ca(HB)_2$ was reported to be lower than that of any other MABs and MHBs, suggesting that the destabilization effect of Ca^{2+} is among the least important ones. Based on such observation, we even concluded that it would be better to consider the binary mixture CaH_2-2HB as hydrogen storage material instead of $Ca(HB)_2$ since the former contains more H atoms (16 versus 12) and releases 2 more equiv H_2 below 90 °C.

4.4. Strontium amidoborane

$Sr(AB)_2$ was prepared by ball milling from strontium hydride SrH_2 and two equivalents of AB [148]. A particular procedure was applied. The reactants were first ball milled at 150 rpm to ensure good homogeneity, and this was done at 0 °C to limit partial decomposition of $Sr(AB)_2$. Then, the mixture was heated at 45 °C for 2 h, allowing faster solid-solid reaction. The final product was not pure. The composition was found to be 55 wt. % of crystalline $Sr(AB)_2$, 34 wt. % of an unidentified amorphous phase, 7 wt. % of SrH_2, and 4 wt. % of AB. An alternative synthesis procedure was developed in which SrH_2 was reacted with two equivalents of AB in THF even though some AB dehydrocoupling onto polymeric products occurred [149].

$Sr(AB)_2$ (Table 4), $Ca(AB)_2$ [148], $Be(AB)_2$ and $Mg(AB)_2$ all crystallize in a monoclinic space group *C*2. Each Sr^{2+} is surrounded by six $[NH_2BH_3]^-$ anions in an octahedral environment. The Sr–N distance is 2.68 Å and the B–N length is 1.53 Å.

The mixture, consisting of 55 wt. % $Sr(AB)_2$, dehydrogenates slowly from 60 °C and violently at 80-90 °C [148]. The weight loss at 200 °C is as high as 9.9 wt. %, which is ca. 3 wt. % higher than the gravimetric H density of $Sr(AB)_2$. This is due to the generation of high amounts of volatile by-products such as NH_3 and B_2H_6. According to computational calculations, the metal ion assisted transfer mechanism and the formation of the transient species Sr_3H drive the initial dehydrogenation step [145]. It was also predicted that $Sr(AB)_2$ would be the most stable of $M(AB)_2$, such as (increasing stability): $Be(AB)_2$ < $Ca(AB)_2$ < $Mg(AB)_2$ < $Sr(AB)_2$ [125], or $Be(AB)_2$ < $Mg(AB)_2$ < $Ca(AB)_2$ < $Sr(AB)_2$ [141]. It is unfortunately perilous to compare such predictions to the experimental results reported above because $Be(AB)_2$ is a virtual compound, $Mg(AB)_2$ and $Ca(AB)_2$ contain small amounts of reactants, and $Sr(AB)_2$ is mixed with 45 wt. % of other products. Such impurities must certainly bias the dehydrogenation results reported for the $M(AB)_2$ compounds.

4.5. Barium amidoborane

$Ba(AB)_2$ was synthesized by wet chemistry in aprotic solvent, in this case THF, by mixing metallic Ba with AB [150]. The reaction is exothermic. The synthesis is preferably performed at low temperature, e.g. at −10 °C, because at higher temperature (e.g. 0 °C) the amidoborane is contaminated by its decomposition products. At −10 °C, an amorphous white precipitate forms. FTIR and ^{11}B MAS NMR spectroscopy confirmed the purity of $Ba(AB)_2$. The dehydrogenation properties of $Ba(AB)_2$ are comparable to those of the other $M(AB)_2$. Between 81 and 163 °C, it loses 5 wt. % of H_2.

5. Materials for hydrogen storage… but not only

5.1. Outlook for hydrogen storage

When a new material is developed for hydrogen storage, one of the properties that is put forward is gravimetric hydrogen storage capacity. For the MABs and MHBs discussed herein, Figure 2 shows the values. The gravimetric hydrogen storage capacities of AB and HB are shown for information.

The weight of the alkali or alkaline earth element has a significant impact on gravimetric hydrogen density (Figure 2). It can therefore be stated, without considering any other argument, that for practical application the potential of the MABs and MHBs made of heavy elements like Rb, Cs, Sr, and Ba is a priori weak (even negligible).

The values listed in Figure 2 are the theoretical (highest) gravimetric hydrogen storage capacities and de facto, they are not realistic [151]. They must be underestimated because of two primary hypotheses. First, partial dehydrogenation of the anions $[NH_2BH_3]^-$ and $[N_2H_3BH_3]^-$ has to be considered in order to avoid formation of a hydrogen-free solid residue like boron nitride of which rehydrogenation is thermodynamically unfavorable [137]. Accordingly, we assume the release of 2 equiv H_2 per $[NH_2BH_3]^-$ or $[N_2H_3BH_3]^-$, which is rather consistent with the experimental data reported in the previous sections. Second, gravimetric hydrogen storage capacity has to be considered on the basis of a storage system taken as a whole, not on the material basis only. Such a system is composed of e.g. tanks, pipes, valves, heaters and electronics, and its weight necessarily affects the weight of the device that has to be powered. In other words, the gravimetric hydrogen storage capacity has to be revised to get the net value while taking into account the weight of the storage system as well. Here, we assume that the system weight is comparable to the weight of the hydrogen storage material, which results in the net gravimetric hydrogen storage capacities shown by the circles in Figure 2. These net capacities confirm the statement made in the previous paragraph, that is, Rb, Cs, Sr, and Ba-based MABs and MHBs have to be excluded for hydrogen storage application.

It has to be admitted that, either way, the Rb, Cs, Sr, and Ba-based MABs and MHBs do not have any tangible proof of benefit in comparison to the other MABs and MHBs. There are several reasons for claiming this. (*i*) Alkali and alkaline earth elements in their metallic state have to be used despite being difficult to handle because of their high reactivity; and, the reaction resulting

in the mentioned derivatives is exothermic which then requires processing at low temperature (e.g. at 0 °C). (*ii*) Their chemical/thermal stability is not high enough. For example, $Sr(AB)_2$ [148] and CsHB [102] evolve during synthesis resulting in a mixture of phases. (*iii*) Under heating, the Rb, Cs, Sr, and Ba-based MABs and MHBs decompose rather than dehydrogenate, with the liberation of substantial amounts of NH_3.

Another argument against the Rb, Cs, Sr, and Ba-based MABs and MHBs is related to the terrestrial abundance of the alkali elements. They, together with Be that in any case has been discarded because of its high toxicity, are scarce in comparison to e.g. Na > K > Li and Ca > Mg.

Ten potential candidates remain for further discussion. These are the Li, Na, K, Mg, and Ca-based MABs and MHBs. Each of the MABs has, comparably to the corresponding MHBs, a higher net gravimetric hydrogen storage capacity (Figure 2). The difference is higher than 1 wt. % H for the Li- and Mg-based compounds; it is close to 1 wt. % H for the Na- and Ca-based materials; and, it is 0.5 wt. % H for KAB versus KHB. Synthesis of MABs requires milder and/or (much) safer conditions (Tables 1 and 2). For example, NaAB can be prepared simply by mixing NaH and AB under inert atmosphere whereas NaHB requires temperatures lower than −30 °C because of the occurrence of an explosive reaction at ambient conditions. Otherwise it should be reiterated that $Mg(HB)_2$ has not been synthesized yet, despite many attempts, and that $Ca(HB)_2$ is the main component of a biphasic mixture obtained in specific conditions. The H_2 generated from the MABs appear to be slightly purer. With the MHBs, H_2 is diluted by some unavoidable N_2 and is systematically polluted by NH_3. The presence of N_2H_4 was even detected with NaHB (Table 4). Assuming that the costs of AB and HB are similar (because synthesized from comparable starting materials and through comparable routes; Tables 1 and 2), the cost of the MABs will be lower than that of the MHBs because of the aforementioned reasons (Figure 13). Based on these arguments, MABs are preferable to MHBs and have a higher application potential.

When reporting their work about $Mg(AB)_2$, Luo et al. [143] used the adjective “long-sought”. The term speaks for itself as it conveys how hard, in fact slow, the reaction between MgH_2 and AB is. With $Mg(AB)_2$, the key is patience: between 45 days and 6 months are required at ambient conditions. With respect to $Ca(AB)_2$, intense milling is required while the reaction between CaH_2

and AB is not complete. In other words, even though both materials have attractive hydrogen capacities, their synthesis hinders their development as hydrogen storage material. Another argument against $Mg(AB)_2$ and $Ca(AB)_2$ is related to their respective dehydrogenation properties. $Mg(AB)_2$ and $Ca(AB)_2$ have to be heated up to 300 and 250 °C respectively to generate about 4 equiv H_2 (2 H_2 per unit of $[NH_2BH_3]^-$ anion). In other words, the recovery of 3.55 and 3.1 wt. % H, corresponding to the net gravimetric hydrogen storage capacities of $Mg(AB)_2$ and $Ca(AB)_2$ respectively, can only be effective at 300 and 250 °C.

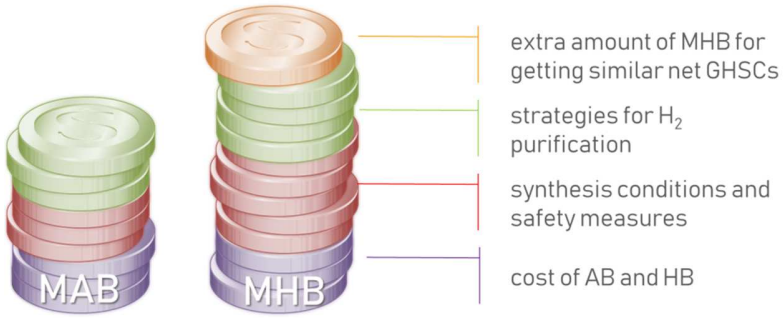

Figure 13. Illustration showing the overall lower cost of the MABs in comparison to that of the MHBs.

The discussion leaves LiAB, NaAB, and KAB. They can be compared by proposing several rankings based on different criteria. (*i*) According to the theoretical and net gravimetric hydrogen storage capacities (Figure 2), the ranking is LiAB > NaAB > KAB. (*ii*) The facile preparation of NaAB (Table 1) and the method based on wet chemistry in aprotic solvent for KAB suggest NaAB > LiAB > KAB. (*iii*) The dehydrogenation properties (extent and kinetics of dehydrogenation) in isothermal conditions are in favor of KAB such as KAB > NaAB > LiAB. (*iv*) The dehydrogenation properties in terms of purity of the released H_2 gives KAB > NaAB ~ LiAB. As it stands, it appears that making a final ranking is difficult, perhaps unwise, especially as other criteria like terrestrial abundancy availability (Na > K >> Li), cost of the alkali element (Na > Li >> K), strong demand because of another commercial use (e.g. Li for batteries), safety issues, and so forth have to be taken into account.

Beyond the criteria mentioned above, it is not possible to make a proper ranking of LiAB, NaAB, and KAB mainly because none of these technologies are mature. Their technological readiness

level (TRL1 to TRL9 [152]) is still low, at the laboratory scale. Research to prove feasibility (TRL3) has been done but, to our knowledge, a technology development (i.e. laboratory testing of "ugly" prototype/storage system; TRL4) has not been considered up to now. In comparison, the technological readiness level of sodium borohydride in hydrolytic conditions is between TRL7 (field test of prototypes) and TRL9 (systems proven in operational environment) and that of AB in thermolysis conditions is between TRL5 (laboratory testing of an integrated system) and TRL7 [153,154].

The screened MABs must climb the TRLs one by one, which implies effort towards scaling up, prototyping, and field-testing. The real potential of e.g. LiAB, NaAB and KAB needs to be evaluated through upscaling.

MABs and MHBs (more widely B-H and B-N-H compounds) suffer from a critical issue: with them, hydrogen storage reversibly is not favorable because dehydrogenation occurs exothermically [74]. The reverse reaction, i.e. rehydrogenation under H_2 pressure, is thermodynamically impossible at affordable conditions [155], and indeed, unsuccessful attempts have been reported for the thermolysis residues forming from LiAB and NaAB. To close the H_2 cycle, the best option is off-board hydrogenation via a chemical reaction [156] in order to form primarily the MAB (or MHB) [136], otherwise AB [138] or sodium borohydride [139]. This is a challenge. It must be said, however, that the number of works towards this objective is restricted to two reports (e.g. refs. [136,138]) in the open literature.

Another issue underpinning the aforementioned challenge is related to residue that is not well identified yet. The difficult identification of the by-products is in fact common to B-N-H compounds. Even with AB that has been investigated more deeply and for a longer period, the exact nature of the residue (forming at different temperatures) remains unclear [155]. Above all, the problem is that the residue is not composed of a single compound and has a complex composition. The ideal would be to decompose AB into polyborazylene only [135]. Maybe we should focus more on "forcing" the dehydrogenation paths that would result in the formation of pure polyborazylene. For that, catalytic modification could be an approach to consider.

Chua et al. [45] suggested catalytic modification as a possible approach to improve the hydrogen storage properties of MABs. This approach obviously deserves to be widely investigated. There may be several benefits: improving the dehydrogenation kinetics; promoting the formation of a single polymeric residue; and, favoring a dehydrogenation route resulting in the release of pure hydrogen. This last point is important, as release of gaseous impurities together with hydrogen has to be solved before these materials find practical applications [74].

Beyond the aforementioned MABs and MHBs, the grand challenge is to develop a new derivative that would dehydrogenate endothermically. This would open the way for direct hydrogenation, under moderate H_2 pressure, of the dehydrogenated residue. Chua et al. [45] suggested focusing on material design. Owarzany et al. [74] mentioned bimetallic amidoborane salts for which thermodynamics of dehydrogenation may be tuned to some extent. Computational chemistry could be necessary for preliminary screenings. In addition, Owarzany et al. suggested other derivatives: for the first one, a halogen would substitute $H^{\delta-}$ of the BH_3 group in $[NH_2BH_3]^-$; for the second one, a carbonaceous chain (alkyl or aryl substituents) would replace $H^{\delta+}$ of NH_2.

Further experimental and computational works, in particular on new derivatives, may help in defining more accurately the chemical bonding properties that would allow taking up all of the challenges described above. Successfully doing this may facilitate designing materials that show the stability requirements mentioned by Wang et al. [72], namely a thermal stability below 40 °C and an ability to decompose above 60 °C.

5.2. Further opportunities

5.2.1. As a reducing agent

The first time that LiAB was discovered in the mid-1990s it was used as a possible reducing agent in organic chemistry. Myers et al. [37] showed that four equivalents of LiAB, freshly prepared in THF at 0 °C, were able to reduce one equivalent of alkylated pseudoephedrine amides at 23 °C resulting in the formation of primary alcohols. Years later, Pasumansky et al. [157] synthesized a series of N-substituted LiAB derivatives ($LiNR^1R^2BH^3$ with R as e.g. H and/or alkyl groups) that were found to reduce aromatic and aliphatic esters, tertiary amides (to

amines or alcohols), α,β-unsaturated aldehydes and ketones (to allylic alcohols), and aliphatic and aromatic azides (to primary amines). Xu et al. [158,159] confirmed the potential of LiAB by reducing, in THF and at room temperature, ketones (e.g. Ph–CO–Ph) to secondary alcohols (e.g. Ph–C(OH)–Ph), and imines (e.g. Ph–CH=N–Ph) to amines (e.g. Ph–CH_2–NH–Ph). NaAB and $Ca(AB)_2$ were successfully used as well. They were also compared to AB and showed different reducing abilities. In a follow-up article, Xu et al. [160] reported the use of LiAB for reductive amination of aldehydes and ketones with primary amines.

AB and more widely amine-boranes had already showed to be attractive reducing agents in e.g. transformation of aldehydes and ketones [163], deracemization of DL-amino acids [164], and conversion of alkenes to amines [165]. In the recent years, with the advent of contemporary "hot" topics, AB and amine-boranes (e.g. $N(CH_3)_2BH_3$) have shown to be effective for reducing metal cations into metal (e.g. Cu, Co) nanoparticles [166,167], graphene oxide into graphene [168,169], and carbon dioxide into valuable chemicals like formic acid and methanol [170,171]. One may then wonder about the use of MABs, as well as of MHBs, instead of AB in similar reactions.

MABs and MHBs are much less soluble in common organic solvents like THF and dioxane than AB is. In protic solvents like water, they are not stable, whereas AB is in neutral and alkaline conditions. These two features therefore limit the use of MABs and MHBs in the aforementioned reactions requiring solvents.

MABs and MHBs, in solid state, are less stable than AB against heating above 50 °C. They may be used instead of AB as potential reducing agents for solid-phase (i.e. solvent-free) synthesis of mono-/multi-metallic nanoparticles. Sanyal and Jagirdar [172,173] showed that AB is able to act as a reducing agent for reducing metal cations and concomitantly as a stabilizing agent for getting nano-sized particles. MABs and MHBs may offer the same roles. In addition, the faster dehydrogenation of these ionic salts at lower temperatures could be advantageous for tuning the nanoparticles size and/or composition. The alkali and alkaline earth cations may also be incuded in the composition of the nanoparticles.

5.2.2. As energetic material

AB (a reducing agent) is able to ignite spontaneously on contact with an oxidizing agent like white fuming nitric acid. It behaves like a hypergolic fuel. Such a potential was first shown by Gao and Shreeve [174] in 2012. However, these authors thought that the solid state of AB is a drawback preventing its ready application. Instead, they developed liquid ionic solutions of AB, and measured ignition delays as short as 3 ms for saturated solutions of AB in reaction with white fuming nitric acid. Interestingly, they also investigated HB and another analog, hydrazine *bis*borane $N_2H_4(BH_3)_2$ (denoted HBB), which dissolved in ionic liquids and showed ignition delays of 3 and 31 ms respectively. In contrast, Ramachandran and co-workers [175-177] saw in the solid state of AB an advantage over the historical hypergolic fuels (i.e. hydrazine and its derivatives). They measured an ignition delay shorter than 10 ms in reaction with fuming nitric acid, hence the authors concluded that solid AB is an interesting hypergolic fuel. In addition to AB, several other amine-boranes (e.g. cyclohexylamine-borane, piperidine-borane and ethylenediamine-*bis*borane) were evaluated as possible hypergolic fuels.

The use of AB as fuel (but not hypergolic) of solid propellant is not so new. Decades ago, AB was proposed as the main component of pellets containing also e.g. Fe_2O_3 or HBB, the obtained propellant being able to release H_2 under ignition (i.e. heating) [178-180]. A comparable use was reported for HB and HBB [181-183]. To a certain extent, these first works are comparable to the recent works dedicated to the H_2 released properties of AB, HB, MABs and MHBs.

MABs and MHBs have been developed to be less stable than AB and HB respectively. They are indeed able to generate H_2 at lower temperature and with faster kinetics. Therefore, they are potential, maybe more attractive, solid fuels of H_2 generating propellants. Given the very fast kinetics reported for e.g. NaHB, the fuel could be tested as a single phase of a propellant ignited by heat. On the other hand, MABs and MHBs are possible hypergolic fuels. Preliminary experiments with white fuming nitric acid, requiring, however, special safe facilities, should allow to explore such a potential.

5.2.3. As boron nitride precursors

There are plenty of potential B- and N- containing precursors of boron nitride BN [184]. A typical example of a precursor is borazine $B_3N_3H_6$. Hirano et al. [185] pyrolyzed it under a

pressure of 100 MPa at 700 °C, which resulted in the formation of amorphous H-containing BN with a yield of 60%. With respect to the Fazen et al.'s approach [186,187], borazine was heated at moderate temperature (70-110 °C) for dehydropolymerization into polyborazylene. The obtained polymer was then pyrolyzed at 900-1500 °C (under argon or ammonia) to produce BN ceramic and chemical yields higher than 83%.

Borazine is the cyclic trimer of AB. It forms in large amounts when pristine AB is heated between 100 and 200 °C. AB is thus also a precursor of BN [188]. For example, Liepins et al. [189] successfully used AB for shock-induced synthesis of cubic BN. Song et al. [190] sublimated AB at 120-130 °C to grow hexagonal BN films by chemical vapor deposition. Kim et al. [191] adopted a two-step process where AB (in tetraglyme) was first catalytically transformed into borazine and, then, the isolated trimer was converted into hexagonal BN films by applying low-pressure chemical vapor deposition. To be brief, AB has shown to be an efficient precursor of BN nanomaterials [192,193] in the form of e.g. layers/films [194,195], and nanotubes [196,197].

With respect to HB, it has not really been considered as a possible precursor of BN, notably because under heating HB decomposes into a shock-sensitive solid residue (Figure 1) [198,199]. HB is however a precursor of BN. Borovinskaya et al. [200] prepared porous BN by self-propagating high-temperature synthesis. Manelis et al. [201], while focusing on the burning rates of HB at 20-100 atm, found that condensed combustion of HB resulted in a fine powder of BN. In a previous study [202], we noticed that HB and AB destabilize each other and that an equimolar mixture of them dehydrogenates, via the formation of an unidentified intermediate and into boron nitride at a temperature as low as 300 °C. In another study [203], we investigated the destabilization of HB by $LiBH_4$ (mol ratio 4:1); upon heating up to 300 °C the binary mixture decomposes into a solid residue of polyborazylene- and/or boron nitride-like materials.

Using pure polyborazylene as a boron nitride precursor, Yuan et al. [204-206] investigated the addition of 5 wt. % of lithium nitride Li_3N. The latter was found to act as a crystallization promoter, allowing a higher crystallization rate and thus low-temperature synthesis of highly crystallized hexagonal boron nitride sheets. The sample heated at 1000 °C was found to be well

crystallized whereas from a promoter-free sample of polyborazylene temperatures higher than 1500 °C are required. This is attractive in terms of energy saving. By exfoliation, the obtained highly crystallized hexagonal boron nitride produced large amounts of self-standing few-layers [207,208]. In previous reports, Li_3N was found to promote the conversion of hexagonal boron nitride into the cubic phase, a dense polytype [209]. To explain the promoter role of Li_3N, it was assumed the formation of melted Li_3BN_2 (Li_3N + BN) as intermediate is able to infiltrate/dissolve hexagonal boron nitride, which results in a recrystallization into cubic boron nitride. Comparably Yuan et al. assumed that Li_3BN_2 forms at 600-700 °C, melts and infiltrates/dissolves amorphous boron nitride, leading then to crystallization of hexagonal boron nitride [204-206].

As for AB and HB, MABs and MHBs may be precursors of boron nitride. They may offer three advantages: (*i*) energy saving owing to the lower temperatures required for dehydrogenation; (*ii*) higher ceramic yield due to evolution of small or negligible amounts of volatile by-products; (*iii*) role of the alkali or alkaline earth element in favoring higher crystallization rates. MABs and MHBs deserve to be investigated in pyrolysis towards the synthesis of boron nitride polytypes.

Focusing on boron nitride is all the more important as boron nitride is likely to belong to the list of reversible hydrogen storage materials. Almost twenty years ago, Wang et al. [210] showed that milled hexagonal boron nitride (crystallites of about 3 nm) adsorbed up to 2.6 wt. % H_2 at 10 bar and room temperature. The uptake of H_2 was reversible since desorption took place at high temperature, namely 297 °C, because of chemisorption. At about the same time, Ma et al. [211] investigated bamboo-like BN nanotubes (210 $m^2\ g^{-1}$) capable of adsorbing up to 2.6 wt. % H_2 under 100 bar and 20 °C, with 0.8 wt. % H_2 being physisorbed. Desorption of the remaining 1.8 wt. % of chemisorbed H_2 required heating up to 300 °C. Such interesting H_2 uptake properties were explained in terms of defects in the nanostructured material, specific surface area, polarity and partial ionic character of the B–N bonds. However, boron nitride has been investigated more scarcely than any other material sorbing H_2 reversibly, which can be explained by a lack of easy approaches of boron nitride synthesis and by a preferential occurrence of H_2 chemisorption [212]. Recently, computational calculations have identified avenues for improving the sorption properties of boron nitride, namely: higher specific surface area [213]; substitution of some B and N atoms of boron nitride by C and/or O [214]; surface functionalization (decoration) with e.g. Li

[215] or Na [216]; 2D boron nitride layers with optimized interlayer spacing [217]. Accordingly, it is reasonable to affirm that MABs and MHBs, especially the Li and Na compounds should be studied as precursors of functionalized boron nitride to be used as reversible hydrogen storage materials. This may open up some interesting horizons for MABs and MHBs.

6. Conclusion

Amidoboranes and hydrazinidoboranes, especially the purely alkali and alkaline earth compounds, have been surveyed in the present review. Many aspects were stressed, including synthesis, crystal structure, gravimetric hydrogen densities, dehydrogenation/decomposition properties and mechanisms, purity of released hydrogen, and nature of polymeric thermolysis residues. From the survey, three conclusions have been drawn as a response to the three features of the title, namely “state of the art”, “potential for hydrogen storage” and “prospects”.

Amidoboranes and hydrazinidoboranes are new materials, mostly discovered within the past decade. Accordingly, they have been investigated scarcely or not sufficiently, and we do not know them well enough. Three examples can be given to illustrate this point: it is not clear if sodium amidoborane releases pure hydrogen or hydrogen together with some ammonia; despite use of computational chemistry, identification of the decomposition intermediates and understanding of the mechanisms are limited; the composition of the dehydrogenation residues is not well isolated, complicating the question of recyclability. The bottom line is that further efforts are required to better understand the amidoboranes and hydrazinidoboranes. This is important from a fundamental point of view, in order to increase our knowledge in the fields of inorganic and materials chemistries. Better knowledge may open up new utilization prospects, beyond chemical hydrogen storage.

Theoretically, amidoboranes and hydrazinidoboranes have a potential for hydrogen storage, which is not confirmed experimentally. Because of scarcity, the compounds carrying the elements like rubidium and cesium are not suitable. Because their synthesis is tough, the calcium and magnesium materials are less attractive. Hydrazinidoboranes release ammonia and/or hydrazine together with hydrogen what make amidoboranes preferable. At the end, when the

theoretical and net gravimetric hydrogen densities are considered, the most suitable compounds seem to be lithium amidoborane, sodium amidoborane and potassium amidoborane. It is however difficult to take the analysis further since none of the mentioned compounds has been scaled up, that is, investigated at the demonstrator scale. It is primordial to dedicate more efforts on scaling up amidoboranes and hydrazinidoboranes in order to increase their technological readiness level. Only in that way will the discussion become decisive and conclusive.

Based on our current knowledge and understanding of amidoboranes and hydrazinidoboranes, we have made three other utilizations emerge. These compounds have relevant prerequisites for other applications, and may be used as solid-state reducing agents, energetic materials, and/or precursors of boron nitride-based ceramics. Specific studies may now be expected.

References

[1] N. Armaroli, V. Balzani. The hydrogen issue. Chem. Sus. Chem. 2011, 4, 21-36.

[2] M. Ball, M. Weeda. The hydrogen economy – Vision or reality? Int. J. Hydrogen Energy 2015, 40, 7903-7919.

[3] T. Sinigaglia, F. Lewiski, M.E.S. Martins, J.C.M. Siluk. Production, storage, fuel stations of hydrogen and its utilization in automotive applications – A review. Int. J. Hydrogen Energy 2017, 42, 24597-24611.

[4] H. Barthelemy, M. Weber, F. Barbier. Hydrogen storage: Recent improvements and industrial perspectives. Int. J. Hydrogen Energy 2017, 42, 7254-7262.

[5] R.K. Ahluwalia, J.K. Peng, H.S. Roh, T.Q. Hua, C. Houchins, B.D. James. Supercritical cryo-compressed hydrogen storage for fuel cell electric buses. Int. J. Hydrogen Energy 2018, 43, 10215-10231.

[6] M.E. Demir, I. Dincer. Cost assessment and evaluation of various hydrogen delivery scenarios. Int. J. Hydrogen Energy 2018, 43, 10420-10430.

[7] P. Jena. Materials for hydrogen storage: past, present, and future. J. Phys. Chem. Lett. 2011, 2, 206-211.

[8] Q. Lai, M. Paskevicius, D.A. Sheppard, C.E. Buckley, A.W. Thornton, M.R. Hill, Q. Gu, J. Mao, Z. Huang, H.K. Liu, Z. Guo, A. Banerjee, S. Chakraborty, R. Ahuja, K.F. Aguey-Zinsou. Hydrogen storage materials for mobile and stationary applications: current state of the art. Chem. Sus. Chem. 2015, 8, 2789-2825.

[9] J. Ren, N.M. Musyoka, H.W. Langmi, M. Mathe, S. Liao. Current research trends and perspectives on materials-based hydrogen storage solutions: a critical review. Int. J. Hydrogen Energy 2017, 42, 289-311.

[10] Á. Berenguer-Murcia, J.P. Marco-Lozar, D. Cazorla-Amorós. Hydrogen storage in porous materials: status, milestones, and challenges. Chem. Rec. 2018, 18, 900-912.

[11] H. Shao, L. He, H. Lin, H.W. Li. Progress and trends in magnesium-based materials for energy-storage research: a review. Energy Technol. 2018, 6, 445-458.

[12] K.C. Kim. A review on design strategies for metal hydrides with enhanced reaction thermodynamics for hydrogen storage applications. Int. J. Energy Res. 2018, 42, 1455-1468.

[13] J. Puszkiel, S. Garroni, C. Milanese, F. Gennari, T. Klassen, M. Dornheim, C. Pistidda. Tetrahydroborates: development and potential as hydrogen storage medium. Inorganics 2017, 5, 74 :1-24.

[14] R. Lan, J.T.S. Irvine, S. Tao. Ammonia and related chemicals as potential indirect hydrogen storage materials. Int. J. Hydrogen Energy 2012, 37, 1482-1494.

[15] G. Moussa, R. Moury, U.B. Demirci, T. Şener, P. Miele. Boron-based hydrides for chemical hydrogen storage. Int. J. Energy Res. 2013, 37, 825-842.

[16] M. Rivarolo, O. Improta, L. Magistri, M. Panizza, A. Barbucci. Thermo-economic analysis of a hydrogen production system by sodium borohydride ($NaBH_4$). Int. J. Hydrogen Energy 2018, 43, 1606-1614.

[17] H.I. Schlesinger, H.C. Brown, A.E. Finholt, J.R. Gilbreath, H.R. Hoekstra, E.K. Hyde. Sodium borohydride, its hydrolysis and its use as a reducing agent and in the generation of hydrogen. J. Am. Chem. Soc. 1953, 75, 215-219.

[18] P. Brack, S.E. Dann, K.G.U. Wijayantha. Heterogeneous and homogenous catalysts for hydrogen generation by hydrolysis of aqueous sodium borohydride ($NaBH_4$) solutions. Energy Env. Eng. 2015, 3, 174-188.

[19] J. Mao, D.H. Gregory. Recent advances in the use of sodium borohydride as a solid state hydrogen store. Energies 2015, 8, 430-453.

[20] D. Ravnsbæk, Y. Filinchuk, Y. Cerenius, H.J. Jakobsen, F. Besenbacher, J. Skibsted, T.R. Jensen. A series of mixed-metal borohydrides. Angew. Chem. Int. Ed. 2009, 48, 6659-6663.

[21] H. Li, Q. Yang, X. Chen, S.G. Shore. Ammonia borane, past as prolog. J. Organomet. Chem. 2014, 751, 60-66.

[22] X. Chen, J.C. Zhao, S.G. Shore. The roles of dihydrogen bonds in amine borane chemistry. Acc. Chem. Res. 2013, 46, 2666-2675.

[23] T. Kar, S. Scheiner. Comparison between hydrogen and dihydrogen bonds among H_3BNH_3, H_2BNH_2, and NH_3. J. Chem. Phys. 2003, 119, 1473-1482.

[24] A. Al-Kukhun, H.T. Hwang, A. Varma, Mechanistic studies of ammonia borane dehydrogenation. Int. J. Hydrogen Energy 2013, 38, 169-179.

[25] U.B. Demirci. Ammonia borane, a material with exceptional properties for chemical hydrogen storage. Int. J. Hydrogen Energy 2017, 42, 9978-10013.

[26] C.W. Hamilton, R.T. Baker, A. Staubitz, I. Manners. B–N compounds for chemical hydrogen storage. Chem. Soc. Rev. 2009, 38, 279-293.

[27] Z. Xiong, C.K. Yong, G. Wu, P. Chen, W. Shaw, A. Karkamkar, T. Autrey, M.O. Jones, S.R. Johnson, P.P. Edwards, W.I.F. David. High-capacity hydrogen storage in lithium and sodium amidoboranes. Nature Mater. 2008, 7, 138-141.

[28] S. Akbayrak, S. Özkar. Ammonia borane as hydrogen storage materials. Int. J. Hydrogen Energy 2018, 43, 18592-18606.

[29] C.H. Liu, Y.C. Wu, C.C. Chou, B.H. Chen, C. L. Hsueh, J.R. Ku, F. Tsau. Hydrogen generated from hydrolysis of ammonia borane using cobalt and ruthenium based catalysts. Int. J. Hydrogen Energy 2012, 37, 2950-2959.

[30] T. Hügle, M.K. Kühnel, D. Lentz. Hydrazine borane: a promising hydrogen storage material. J. Am. Chem. Soc. 2009, 131, 7444-7446.

[31] S. Karahan, M. Zahmakiran, S. Özkar. Catalytic hydrolysis of hydrazine borane for chemical hydrogen storage: highly efficient and fast hydrogen generation system at room temperature. Int. J. Hydrogen Energy 2011, 36, 4958-4966.

[32] J. Hannauer, O. Akdim, U.B. Demirci, C. Geantet, J.M. Herrmann, P. Miele, Q. Xu. High-extent dehydrogenation of hydrazine borane $N_2H_4BH_3$ by hydrolysis of BH_3 and decomposition of N_2H_4. Energy Environ. Sci. 2011, 4, 3355-3358.

[33] Q.L. Zhu, D.C. Zhong, U.B. Demirci, Q. Xu. Controlled synthesis of ultrafine surfactant-free NiPt nanocatalysts toward efficient and complete hydrogen generation from hydrazine borane at room temperature. ACS Catal. 2014, 4, 4262-4268.

[34] R. Moury, U.B. Demirci. Hydrazine borane and hydrazinidoboranes as chemical hydrogen storage materials. Energies 2015, 8, 3118-3141.

[35] H.I. Schlesinger, A.B. Burg. Hydrides of boron. VIII. The structure of the diammoniate of diborane and its relation to the structure of diborane. J. Am. Chem. Soc. 1938, 60, 290-299.

[36] H.I. Schlesinger, A.B. Burg. Recent developments in the chemistry of the boron hydrides. Chem. Rev. 1942, 31, 1-41.

[37] A.G. Myers, B.H. Yang, D.J. Kopecky. Lithium amidotrihydroborate, a powerful new reductant. Transformation of tertiary amides to primary alcohols. Tetrahedron Lett. 1996, 37, 3623-3626.

[38] H.V.K. Diyabalanage, R.P. Shrestha, T.A. Semelsberger, B.L. Scott, M.E. Bowden, B.L. Davis, A.K. Burrell. Calcium amidotrihydroborate: a hydrogen storage material. Angew. Chem. Int. Ed. 2007, 46, 8995-8997.

[39] J. Spielman, G. Jansen, H. Bandmann, S. Harder. Calcium amidoborane hydrogen storage materials: crystal structures of decomposition products. Angew. Chem. Int. Ed. 2008, 47, 6290-6295.

[40] C. Wu, G. Wu, Z. Xiong, X. Han, H. Chu, T. He, P. Chen. $LiNH_2BH_3{\cdot}NH_3BH_3$: structure and hydrogen storage properties. Chem. Mater. 2010, 22, 3-5.

[41] W. Li, R.H. Scheider, C.M. Araújo, G. Wu, A. Blomqvist, C. Wu, R. Ahuja, Y.P. Feng, P. Chen. Understanding from first-principles why $LiNH_2BH_3{\cdot}NH_3BH_3$ shows improved dehydrogenation over $LiNH_2BH_3$ and NH_3BH_3. J. Phys. Chem. C 2010, 114, 19089-10905.

[42] G. Xia, X. Yu, Y. Guo, Z. Wu, C. Yang, H. Liu, S. Dou. Amminelithium amidoborane $Li(NH_3)NH_2BH_3$: a new coordination compound with favorable dehydrogenation characteristics. Chem. Eur. J. 2010, 16, 3763-3769.

[43] Y.S. Chua, G.T. Wu, Z.T. Xiong, A. Karkamkar, J.P. Guo, M.X. Jian, M.W. Wong, T. Autrey, P. Chen. Synthesis, structure and dehydrogenation of magnesium amidoborane monoammoniate. Chem. Commun. 2010, 46, 5752-5754.

[44] Y.S. Chua, G.T. Wu, Z.T. Xiong, T. He, P. Chen. Calcium amidoborane ammoniate – Synthesis, structure, and hydrogen storage properties. Chem. Mater. 2009, 21, 4899-4904.

[45] Y.S. Chua, P. Chen, G. Wu, Z. Xiong. Development of amidoboranes for hydrogen storage. Chem. Commun. 2011, 47, 5116-5129.

[46] T. He, H. Wu, G. Wu, Z. Li, W. Zhou, X. Ju, D. Xie, P. Chen. Lithium amidoborane hydrazinates: synthesis, structure and hydrogen storage properties. J. Mater. Chem. A 2015, 3, 10100-10106.

[47] Z. Li, T. He, G. Wu, W. Chen, Y.S. Chua, J. Guo, D. Xie, X. Ju, P. Chen. Synthesis, structure and the dehydrogenation mechanism of calcium hydrazinates. Phys. Chem. Chem. Phys. 2016, 18, 244-251.

[48] R.V. Genova, K.J. Fijalkowski, A. Budzianowski, W. Grochala. Towards $Y(NH_2BH_3)_3$: probing hydrogen storage properties of YX_3/NH_2BH_3 (X = F, Cl; M = Li, Na) and $YH_{x\sim3}/NH_3BH_3$ composites. J. Alloys Compd. 2010, 499, 144-148.

[49] M.F. Hawthorne, S.S. Jalisatgi, A.V. Safronov, H.B. Lee, J. Wu. Chemical hydrogen storage using polyhedral borane anions and aluminum-ammonia-borane complexes; Final report; University of Missouri. 2010. Available online: http://www.osti.gov/scitech//servlets/purl/990217-xUxbgx/ (accessed on June 2019).

[50] S.S. Jalisatgi, J. Wu, M.F. Hawthorne, M.F. Chemical hydrogen storage using aluminum ammonia-borane complexes; Report, University of Missouri. 2009. Available online: https://www.hydrogen.energy.gov/pdfs/review09/stp_20_hawthorne.pdf (accessed on June 2019).

[51] A.L. DeGraffenreid. Studies on boron-nitrogen and boron-gadolinium compounds. Ph.D. thesis, The Ohio State University, Columbus, OH, USA, 1995.

[52] R. Owarzany. Synthesis and characterization of zinc amidoborane. Bachelor's thesis, University of Warsaw, Warsaw, Poland, 2013.

[53] L.H. Rude, T.K. Nielsen, D.B. Ravnsbæk, U. Bösenberg, M.B. Ley, B. Richter, L.M. Arnbjerg, M. Dornheim, Y. Filinchuk, F. Besenbacher, T.R. Jensen. Tailoring properties of borohydrides for hydrogen storage: a review. Phys. Stat. Solid. A 2011, 208, 1754-1773.

[54] Y. Zhang, K. Shimoda, T. Ichikawa, Y. Kojima. Activation of ammonia borane hybridized with alkaline-metal hydrides: a low-temperature and high-purity hydrogen generation material. J. Phys. Chem. 2010, 114, 14662-14664.

[55] X. Kang, J. Luo, Q. Zhang, P. Wang. Combined formation and decomposition of dual-metal amidoborane $NaMg(NH_2BH_3)_3$ for high-performance hydrogen storage. Dalton Trans. 2011, 40, 3799-3801.

[56] K.J. Fijalkowski, R.V. Genova, Y. Filinchuk, A. Budzianowski, M. Derzsi, T. Jaroń, P.J. Leszczyński, W. Grochala. $Na[Li(NH_2BH_3)_2]$ – The first mixed-cation amidoborane with unusual crystal structure. Dalton Trans. 2011, 40, 4407-4413.

[57] H. Wu, W. Zhou, F.E. Pinkerton, M.S. Meyer, O. Yao, S. Gadipelli, T.J. Udovic, T. Yildirim, J.J. Rush. Sodium magnesium amidoborane: the first mixed-metal amidoborane. Chem. Commun. 2011, 47, 4102-4104.

[58] X.D. Kang, J.H. Luo, P. Wang. Efficient and highly rapid hydrogen release from ball-milled $3NH_3BH_3/MMgH_3$ (M [Na, K, Rb]) mixtures at low temperatures. Int. J. Hydrogen Energy 2012, 37, 4259-4266.

[59] W. Li, L. Miao, R.H. Scheicher, Z. Xiong, G. Wu, C.M. Araújo, A. Blomqvist, R. Ahuja, Y. Feng, P. Chen. Li-Na ternary amidoborane for hydrogen storage: experimental and first-principles study. Dalton Trans. 2012, 41, 4754-4764.

[60] K. Wang, J.G. Zhang, P. He. Theoretical study on the structure and dehydrogenation mechanism of mixed metal amidoborane, $Na[Li(NH_2BH_3)]_2$. J. Alloys Compd. 2013, 581, 59-65.

[61] Y.S. Chua, W. Li, G.T. Wu, Z.T. Xiong, P. Chen. From exothermic to endothermic dehydrogenation – Interaction of monoammoniate of magnesium amidoborane and metal hydrides. Chem. Mater. 2012, 24, 3574-3581.

[62] G. Xia, Y. Tan, X. Chen, Z. Guo, H. Liu, X. Yu. Mixed-metal (Li, Al) amidoborane: synthesis and enhanced hydrogen storage properties. J. Mater. Chem. A 2013, 1, 1810-1820.

[63] I. Dovgaliuk, L.H. Jepsen, D.A. Safin, Z. Łodziana, V. Dyadkin, T.R. Jensen, M. Devillers, Y. Filinchuk. A composite of complex and chemical hydrides yields the first Al-based amidoborane with improved hydrogen storage properties. Chem. Eur. J. 2015, 21, 14562-14570.

[64] K. Wang, J.G. Zhang, T. Li, Y. Liu, T. Zhang, Z.N. Zhou. Electronic structures and dehydrogenation properties of bimetallic amidoboranes. Int. J. Hydrogen Energy 2015, 40, 2500-2508.

[65] Y. Nakagawa, K. Shintazo, T. Nakagawa, K. Nakajima, S. Isobe, K. Goshome, H. Miyaoka, T. Ichikawa. Synthesis, structural characterization, and hydrogen desorption properties of $Na[Al(NH_2BH_3)_4]$. Int. J. Hydrogen Energy 2017, 42, 6173-6180.

[66] N. Biliškov, A. Borgschulte, K. Užarević, I. Halasz, S. Lukin, S. Milošević, I. Milanović, J.G. Novaković. In-situ and real-time monitoring of mechanochemical preparation of $Li_2Mg(NH_2BH_3)_4$ and $Na_2Mg(NH_2BH_3)_4$ and their thermal dehydrogenation. Chem. Eur. J. 2017, 23, 16274-16282.

[67] C.H. Lee, Y. Nakagawa, S. Isobe, N. Hashimoto, S. Sugio, H. Miyaoka, T. Ichikawa. Synthesis of sodium-magnesium amidoborane by sodium amide: an investigation of functional properties for hydrogen/ammonia storage. J. Alloys Compd. 2019, 801, 645-650.

[68] A.M. Chernysheva, P.A. Shelyganov, I.V. Kazakov, A.Y. Timoshkin. Complex amidoboranes $M^2[M^1(NH_2BH_3)_4]$ (M^1 = Al, Ga; M^2 = Li, Na, K, Rb, Cs). Russ. J. Gen. Chem. 2017, 87, 665-669.

[69] K.T. Møller, M. Jørgensen, J.G. Andreasen, J. Skibsted, Z. Łodziana, Y. Filinchuk, T.R. Jensen. Synthesis and thermal decomposition of potassium tetraamidoboranealuminate $K[Al(NH_2BH_3)_4]$. Int. J. Hydrogen Energy 2018, 43, 311-321.

[70] D.J. Wolstenholme, J. Flogeras, F.N. Che, A. Decken, G.S. McGrady. Homopolar dihydrogen bonding in alkali metal amidoboranes: crystal engineering of low-dimensional molecular materials. J. Am. Chem. Soc. 2013, 135, 2439-2442.

[71] T.D. Forster, H.M. Tuononen, M. Parvez, R. Roesler. Characterization of β-B-agostic isomers in zirconocene amidoborane complexes. J. Am. Soc. Chem. 2009, 131, 6689-6691.

[72] G. Alcaraz, S. Sabo-Etienne. Coordination and dehydrogenation of amine-boranes at metal centers. Angew. Chem. Int. Ed. 2010, 49, 7170-7179.

[73] K. Wang, J.G. Zhang, T.T. Man, M. Wu, C.C. Chen. Recent progress and development of metal amidoborane. Chem. Asian J. 2013, 8, 1076-1089.

[74] R. Owarzany, P.J. Leszczyński, K.J. Fijalkowski, W. Grochala. Mono- and bimetallic amidoboranes. Crystals 2016, 6, 88.

[75] T.E. Stennett, S. Harder. s-Block amidoboranes: syntheses, structures, reactivity and applications. Chem. Soc. Rev. 2016, 45, 1112-1128.

[76] A. Rossin, M. Peruzzini. Ammonia-borane and amine-borane dehydrogenation mediated by complex metal hydrides. Chem. Rev. 2016, 116, 8848-8872.

[77] K. Wang, Z. Pan, X. Yu. Metal B-N-H hydrogen-storage compound: development and perspective. J. Alloys Compd. 2019, 794, 303-324.

[78] N.J. Hess, M.E. Bowden, V.M. Parvanov, C. Mundy, S.M. Kathmann, G.K. Schenter, T. Autrey. Spectroscopic studies of the phase transition in ammonia borane: Raman spectroscopy of single crystal NH_3BH_3 as a function of temperature from 88 to 330 K. J. Phys. Chem. 2008, 128, 034508.

[79] R. Moury, G. Moussa, U.B. Demirci, J. Hannauer, S. Bernard, E. Petit, A. van der Lee, P. Miele. Hydrazine borane: synthesis, characterization, and application prospects in chemical hydrogen storage. Phys. Chem. Chem. Phys. 2012, 14, 1768–1777.

[80] A.K. Figen, M.B. Pişkin, B. Coşkuner, V. Imamoğlu. Synthesis, structural characterization, and hydrolysis of ammonia borane (NH_3BH_3) as a hydrogen storage carrier. Int. J. Hydrogen Energy 2013, 38, 16215-16228.

[81] M.G. Hu, R.A. Geanangel, W.W. Wendlandt. The thermal dissociation of ammonia borane. Thermochim. Acta. 1978, 23, 249-255.

[82] S. Sit, R.A. Geanangel, W.W. Wendlandt. The thermal dissociation of NH_3BH_3. Thermochim. Acta. 1987, 113, 379-382.

[83] F. Baitalow, J. Baumann, G. Wolf, K. Jaenicke-Rößler, G. Leitner. Thermal decomposition of B–N–H compounds investigated by using combined thermoanalytical methods. Thermochim. Acta 2002, 391, 159-168.

[84] C. Wu, G. Wu, Z. Xiong, W.I.F. David, K.R. Ryan, M.O. Jones, P.P. Edwards, H. Chu, P. Chen. Stepwise phase transition in the formation of lithium amidoborane. Inorg. Chem. 2010, 49, 4319-4323.

[85] H. Wu, W. Zhou, T. Yildirim. Alkali and alkaline-earth metal amidoboranes: structure, crystal chemistry, and hydrogen storage properties. J. Am. Chem. Soc. 2008, 130, 14834-14839.

[86] K.J. Fijalkowski, R. Jurczakowski, W. Koźmiński, W. Grochala. Insights from impedance spectroscopy into the mechanism of thermal decomposition of $M(NH_2BH_3)$, M = H, Li, Na, $Li_{0.5}Na_{0.5}$, hydrogen stores. Phys. Chem. Chem. Phys. 2012, 14, 5778-5784.

[87] A.T. Luedtke, T. Autrey. Hydrogen release studies of alkali amidoboranes. Inorg. Chem. 2010, 49, 3905-3910.

[88] G. Xia, J. Chen, W. Sun, Y. Tan, Z. Guo, H. Liu, X. Yu. Well-dispersed lithium amidoborane nanoparticles through nanoreactor engineering for improved hydrogen release. Nanoscale 2014, 6, 12333-12339.

[89] K. Shimoda, Y. Zhang, T. Ichikawa, H. Mitaoka, Y. Kojima. Solid state NMR study on the thermal decomposition pathway of sodium amidoborane $NaNH_2BH_3$. J. Mater. Chem. 2011, 21, 2609-2615.

[90] K.J. Fijałkowski, W. Grochala. Substantial emission of NH_3 during thermal decomposition of sodium amidoborane, $NaNH_2BH_3$. J. Mater. Chem. 2009, 19, 2043-2050.

[91] Z. Xiong, G. Wu, Y.S. Chua, J. Hu, T. He, W. Xu, P. Chen. Synthesis of sodium amidoborane ($NaNH_2BH_3$) for hydrogen production. Energy Environ. Sci. 2008, 1, 360-363.

[92] F.P.R. Sandra, U.B. Demirci, R. Chiriac, R. Moury, P. Miele. A simple preparation method of sodium amidoborane, highly efficient derivative of ammonia borane dehydrogenating at low temperature. Int. J. Hydrogen Energy 2011, 36, 7423-7430.

[93] H.V.K. Diyabalanage, T. Nakagawa, R.P. Shrestha, T.A. Semelsberger, B.L. Davis, B.L. Scott, A.K. Burrell, W.I.F. David, K.R. Ryan, M.O. Jones, P.P. Edwards. Potassium(I) amidotrihydroborate: structure and hydrogen release. J. Am. Chem. Soc. 2010, 132, 11836-11837.

[94] I.V. Kazakov, A.V. Butlak, P.A. Shelyganov, V.V. Suslonov, A.Y. Timoshkin. Reversible structural transformation of rubidium and cesium amidoboranes. Polyhedron 2017, 127, 186-190.

[95] R. Owarzany, T. Jaroń, P.J. Leszczyński, K.J. Fijalkowski, W. Grochala. Amidoborane of rubidium and caesium: the last missing members of the alkali metal amidoborane family. Dalton Trans. 2017, 46, 16315-16320.

[96] H. Wu, W. Zhou, F.E. Pinkerton, T.J. Udovic, T. Yildirim, J.J. Rush. Metal hydrazinoborane $LiNH_2BH_3$ and $LiNH_2BH_3{\cdot}2N_2H_4BH_3$: crystal structures and high-extent dehydrogenation. Energy Environ. Sci. 2012, 5, 7531-7355.

[97] R. Moury, U.B. Demirci, V. Ban, Y. Filinchuk, T. Ichikawa, L. Zeng, K. Goshome, P. Miele. Lithium hydrazinidoborane: a polymorphic material with potential for chemical hydrogen storage. Chem. Mater. 2014, 26, 3249-3255.

[98] Y.S. Chua, Q. Pei, X. Ju, W. Zhou, T.J. Udovic, G. Wu, Z. Xiong, P. Chen, H. Wu. Alkali metal hydride modification on hydrazine borane for improved dehydrogenation. J. Phys. Chem. C 2014, 118, 11244-11251.

[99] Y. Tan, X. Chen, J. Chen, Q. Gu, X. Yu. The decompositon of α-$LiN_2H_3BH_3$: an unexpected hydrogen release from a homopolar proton-proton pathway. J. Mater. Chem. A 2014, 2, 15627-15632.

[100] R. Moury, U.B. Demirci, T. Ichikawa, Y. Filinchuk, R. Chiriac, A. van der Lee, P. Miele. Sodium hydrazinidoborane: a chemical hydrogen-storage material. Chem. Sus. Chem. 2013, 6, 667-673.

[101] C.A. Castilla-Martinez, D. Granier, C. Charmette, G. Maurin, P.G. Yot, U.B. Demirci. Rubidium hydrazinidoborane: synthesis, characterization and hydrogen release properties. Int. J. Hydrogen Energy 2019, 44, 28252-28261.

[102] C.A. Castilla-Martinez, D. Granier, C. Charmette, J. Cartier, P.G. Yot, U.B. Demirci. Cesium hydrazinidoborane, the last of the alkali hydrazinidoboranes, studied as potential hydrogen storage material. Int. J. Hydrogen Energy 2020, accepted.

[103] S. Harder. Molecular early main group metal hydrides: synthetic challenge, structures and applications. Chem. Commun. 2012, 48, 11165-11177.

[104] S. Pylypko, J.F. Petit, S. Ould-Amara, N. Hdhili, A. Taihei, R. Chiriac, T. Ichikawa, M. Cretin, P. Miele, U.B. Demirci. Metal hydride-hydrazine borane: towards hydrazinidoboranes or composites as hydrogen carriers. Int. J. Hydrogen Energy 2015, 40, 14875-14884.

[105] I. Milanovic, N. Biliskov. Mechanochemical pretreatment of ammonia borane: a new procedure for sodium amidoborane synthesis. Int. J. Hydrogen Energy 2010, 45, 7938-7946.

[106] M.A. Bowden, G.J. Gainsford, W.T. Robinson. Room-temperature structure of ammonia borane. Aust. J. Chem. 2007, 60, 149-153.

[107] R. Moury, K. Robeyns, Y. Filinchuk, P. Miele, U.B. Demirci. *In situ* thermodiffraction to monitor synthesis and thermolysis of hydrazine borane-based materials. J. Alloys Compd. 2016, 659, 210-216.

[108] P.G. Yot, P. Miele, U.B. Demirci. *In situ* synchrotron X-ray thermodiffraction of boranes. Crystals 2016, 6, 16.

[109] M. Ramzan, F. Silverav, A. Blomqvist, R.H. Scheicher, S. Lebègue, R. Ahuja. Structural and energetic analysis of the hydrogen storage materials $LiNH_2BH_3$ and $NaNH_2BH_3$ from *ab initio* calculation. Phys. Rev. B 2009, 79, 132102.

[110] A C. Stowe, W.J. Shaw, J.C. Linehan, B. Schmid, T. Autrey. *In situ* solid state ^{11}B MAS-NMR studies of the thermal decomposition of ammonia borane: mechanistic studies of the hydrogen release pathways from a solid state hydrogen storage material. Phys. Chem. Chem. Phys. 2007, 9, 1831-1836.

[111] W.T. Klooster, T.F. Koetzle, P.E.M. Siegbahn, T.B. Richardson, R.H. Crabtree. Study of the N-H···H-B dihydrogen bond including the crystal structure of BH_3NH_3 by neutron diffraction. J. Am. Chem. Soc. 1999, 121, 6337-6343.

[112] D.J. Wolstenholme, J.T. Titah, F.N. Che, K.T. Traboulsee, J. Flogeras, G.S. McGrady. Homopolar dihydrogen bonding in alkali-metal amidoboranes and its implications for hydrogen storage. J. Am. Chem. Soc. 2011, 133, 16598-16604.

[113] S. Najiba, J. Chen, High-pressure study of lithium amidoborane using Raman spectroscopy and insight into dihydrogen bonding absence, Proc. Natl Acad. Sci. 2012, 109, 19140-19144.

[114] L. Liu, s. Wang, Y. Wu, Z. Li, L. Jiang, X. Guo, J. Ye, Dehydrogenation of two phases of $LiNH_2BH_3$. Int. J. Hydrogen Energy 2020, 45, 2127-2134.

[115] K. Shimoda, K. Doi, T. Nakagawa, Y. Zhang, H. Miyaoka, T. Ichikawa, M. Tansho, T. Shimizu, A.K. Burrell, Y. Kojima. Comparative study of structural changes in NH_3BH_3, $LiNH_2BH_3$, and KNH_2BH_3 during dehydrogenation process. J. Phys. Chem. C 2012, 116, 5957-5964.

[116] K.Wang, J. Zhang, T. Zhang. Crystal and electronic structures of solid $M(NH_2BH_3)_n$ (M = Li, Na, K) and the decomposition mechanisms. Int. J. Hydrogen Energy 2014, 39, 21372-21379.

[117] Y. Zhang, C. Wolverton. Crystal structures, phase stabilities, and hydrogen storage properties of metal amidoboranes. J. Phys. Chem. C 2012, 116, 14224-14231.

[118] R. Moury, J.F. Petit, U.B. Demirci, T. Ichikawa, P. Miele. Pure hydrogen-generating “doped” sodium hydrazinidoborane. Int. J. Hydrogen Energy 2015, 40, 7475-7482.

[119] M. Bowden, D.J. Heldebrant, A. Karkamkar, T. Proffen, G.K. Schenter, T. Autrey. The diammoniate of diborane: crystal structure and hydrogen release. Chem. Commun. 2010, 46, 8564-8566.

[120] S.A. Shevlin, B. Kerkeni, Z.X. Guo. Dehydrogenation mechanisms and thermodynamics of MNH_2BH_3 (M = Li, Na) metal amidoboranes as predicted from first principles. Phys. Chem. Chem. Phys. 2011, 13, 7649-7459.

[121] Y. Zhang, T. Autrey, C. Wolverton. First-principles prediction of intermediate products in the decomposition of metal amidoboranes. J. Phys. Chem. C 2012, 116, 26728-26734.

[122] D.Y. Kim, N.J. Singh, H.M. Lee, K.S. Kim. Hydrogen-release mechanisms in lithium amidoboranes. Chem. Eur. J. 2009, 15, 5598-5604.

[123] S. Swinnen, V.S. Nguyen, M.T. Nguyen. Potential hydrogen storage of lithium amidoboranes and derivatives. Chem. Phys. Lett. 2010, 489, 148-153.

[124] K.R. Ryan, A.J. Ramirez-Cuesta, K. Refson, M.O. Jones, P.P. Edwards, W.I.F. David. A combined experimental inelastic neutron scattering, Raman and *ab initio* lattice dynamics study of α-lithium amidoborane. Phys. Chem. Chem. Phys. 2011, 13, 12249-12253.

[125] D.Y. Kim, D.Y. Kim, J. Seo, S.K. Shin, K.S. Kim. Rules and trends of metal cation driven hydride-transfer mechanisms in metal amidoboranes. Phys. Chem. Chem. Phys. 2010, 12, 5446-5453.

[126] T. Li, J.G. Zhang. Theoretical study of the metal-controlled dehydrogenation mechanism of $MN_2H_3BH_3$ (M = Li, Na, K): a new family of hydrogen storage material. J. Phys. Chem. A 2018, 122, 1344-1349.

[127] A.V. Pomogaeva, K. Morokuma, A.Y. Timoshkin. Trimeric cluster of lithium amidoborane – the smallest unit for the modeling of hydrogen release mechanism. J. Comput. Chem. 2016, 37, 1259-1264.

[128] A.V. Pomogaeva, K. Morokuma, A.Y. Timoshkin. Mechanisms of hydrogen generation from tetrameric clusters of lithium amidoborane. J. Phys. Chem. A 2016, 120, 145-152.

[129] T. Banu, K. Sen, T. Ash, A.K. Das. Dehydrogenation of lithium hydrazinidoborane: insight from computational analysis. Int. J. Hydrogen Energy 2016, 41, 18953-18962.

[130] K.J. Fijalkowski, T. Jaroń, P.J.. Leszczyński, E. Magos-Palasyuk, T. Palasyuk, M.K. Cyrański, W. Grochala. $M(BH_3NH_2BH_2NH_2BH_3)$ – The missing link in the mechanism of the thermal decomposition of light alkali metal amidoboranes. Phys. Chem. Chem. Phys. 2014, 16, 23340-23346.

[131] T. Li, K. Wang, J.G. Zhang. Theoretical study of the structure and dehydrogenation mechanism of sodium hydrazinidoborane. J. Theor. Comput. Chem. 2017, 16, 1750020.

[132] D.J. Wolstenholme, K.T. Traboulsee, Y. Hua, L. Calhoun, G.S. McGrady. Thermal desorption of hydrogen from ammonia borane: unexpected role of homopolar B–H···H–B interactions. Chem. Commun. 2012, 48, 2597-2599.

[133] B. Roy, A. Hajari, J. Manna, P. Sharma. Supported ammonia borane decomposition through enhanced homopolar B–B coupling. Dalton Trans. 2018, 47, 6570-6579.

[134] J.F. Petit, U.B. Demirci. Mechanistic insights into dehydrogenation of partially deuterated ammonia borane NH_3BD_3 being heating to 200°C. Inorg. Chem. 2019, 58, 489-494.

[135] A.D. Sutton, A.K. Burrell, D.A. Dixon, E.B. Garner III, J.C. Gordon, T. Nakagawa, K.C. Ott, J.P. Robinson, M. Vasiliu. Regeneration of ammonia borane spent fuel by direct reaction with hydrazine and liquid ammonia. Science 2011, 331, 1426-1429.

[136] Z. Tang, Y. Tan, X. Chen, X. Yu. Regenerable hydrogen storage in lithium amidoborane. Chem. Commun. 2012, 48, 9296-9298.

[137] J. Eichler, C. Lesniak. Boron nitride (BN) and BN composites for high-temperature applications. J. Eur. Ceram. Soc. 2008, 28, 1105-1109.

[138] Z. Tang, L. Zhang, L. Wan, Z. Huang, H. Liu, Z. Guo, X. Yu. Regeneration of alkaline metal amidoboranes with high purity. Int. J. Hydrogen Energy 2016, 41, 407-412.

[139] L. Ouyang, H. Zhong, H.W. Li, M. Zhu. A recycling hydrogen supply system of $NaBH_4$ based on a facile regeneration process: a review. Inorganics 2018, 6, 10.

[140] E.I. Davydova, A.S. Lisovenko, A.Y. Timoshkin. Complex beryllium amidoboranes: structures, stability, and evaluation of their potential as hydrogen storage materials. J. Comput. Chem. 2017, 38, 401-405.

[141] A.S. Lisovenko, A.Y. Timoshkin. Formation and unimolecular dehydrogenation of gaseous alkaline-earth metal amidoboranes $M(NH_2BH_3)_2$ (M = Be – Ba): comparative computational study. Z. Anorg. Allg. Chem. 2017, 643, 209-213.

[142] Y. Nakagawa, S. Isobe, Y. Ikarashi, S. Ohnuki. AB-MH (ammonia borane-metal hydride) composites: systematic understanding of dehydrogenation properties. J. Mater. Chem. A 2014, 2, 3926-3931.

[143] J. Luo, X. Kang, P. Wang. Synthesis, formation mechanism, and dehydrogenation properties of the long-sought $Mg(NH_2BH_3)_2$ compound. Energy Environ. Sci. 2013, 6, 1018-1025.

[144] K. Wang, V. Arcisauskaite, J.S. Jiao, J.G. Zhang, T.L. Zhang, Z.N. Zhou. Structural prediction, analysis and decomposition mechanism of solid $M(NH_2BH_3)_n$ (M = Mg, Ca and Al). RSC Adv. 2014, 4, 14624-14632.

[145] A.V. Pomogaeva, A.Y. Timoshkin. Initial steps for the thermal decomposition of alkaline-earth metal amidoboranes: a cluster approximation. Phys. Chem. Chem. Phys. 2016, 18, 31072-31077.

[146] F. Leardini, J.R. Ares, J. Bodega, M.J. Valero-Pedraza, M.A. Bañares, F.F. Fernández, C. Sánchez. Hydrogen desorption behavior of calcium amidoborane obtained by reactive milling of calcium hydride and ammonia borane. J. Phys. Chem. C 2012, 116, 24430-24435.

[147] S. Ould-Amara, V. Yadav, E. Petit, G. Maurin, P.G. Yot, U.B. Demirci. Calcium hydrazinidoborane: synthesis, characterizations, and promises for hydrogen storage. Int. J. Hydrogen Energy 2020, 45, 2022-2033.

[148] Q. Zhang, C. Tang, C. Fang, F. Fang, D. Sun, L. Ouyang, M. Zhu. Synthesis, crystal structure, and thermal decomposition of strontium amidoborane. J. Phys. Chem. C 2010, 114, 1709-1714.

[149] Yu.V. Kondrat'ev, A.V. Butlak, I.V. Kazakov, I.S. Krasnova, M.V. Chislov, A.Yu. Timoshkin. Heat effects of the thermal decomposition of amidoboranes of potassium, calcium, and strontium. Russ. J. Phys. Chem. A 2018, 92, 640-645.

[150] N.A. Shcherbina, I.V. Kazakov, A.Yu. Timoshkin. Synthesis and characterization of barium amidoborane. Russ. J. Gen. Chem. 2017, 87, 2875-2877.

[151] J. Yang, A. Sudik, C. Wolverton and D. J. Siegel. High capacity hydrogen storage materials: attributes for automotive applications and techniques for materials discovery. Chem. Soc. Rev. 2010, 39, 656-675.

[152] J.C. Mankins. Technology readiness assessments: A retrospective. Acta Astronaut 2009, 65, 1216-23.

[153] U.B. Demirci. About the technological readiness of the H_2 generation by hydrolysis of B(-N)-H compounds. Energy Technol 2018, 6, 470-86.

[154] J.E. Seo, Y. Kim, Y. Kim, K. Kim, J.H. Lee, D.H. Lee, Y. Kim, S.J. Shin, D.M. Kim, S.Y. Kim, T. Kim, C.W. Yoon, S.W. Nam. Portable ammonia-borane-based H_2 power-pack for unmanned aerial vehicles. J Power Sources 2014, 254, 329-337.

[155] O.T. Summerscales, J.C. Gordon. Regeneration of ammonia borane from spent fuel materials. Dalton Trans. 2013, 42, 10075-10084.

[156] N.C. Smythe, J.C. Gordon. Ammonia borane as a hydrogen carrier: dehydrogenation and regeneration. Eur. J. Inorg. Chem. 2010, 4, 509-521.

[157] L. Pasumansky, C.T. Goralski, B. Singaram, Lithium aminoborohydrides: powerful, selective, air-stable reducing agents, Org. Process Res. Dev. 2006, 10, 959-970.

[158] W. Xu, G. Wu, W. Yao, H. Fan, J. Wu, P. Chen, Metal amidoboranes: superior double-hydrogen-transfer agents in the reduction of ketones and imines, Chem. Eur. J. 2012, 18, 13885-13892.

[159] W. Xu, Y. Zhou, R. Wang, G. Wu, P. Chen, Lithium amidoborane, a highly chemoselective reagent for the reduction of α,β-unsaturated ketones to allylic alcohols, Org. Biomol. Chem. 2012, 10, 367-371.

[160] W. Xu, X. Zheng, G. Wu, P. Chen, Reductive amination of aldehydes and ketones with primary amines by using lithium amidoborane as reducing reagent, Chin. J. Chem. 2012, 30, 1775-1780.

[161] G.C. Andrews, T.C. Crawford, The synthetic utility of amine borane reagents in the reduction of aldehydes and ketones, Tetrahedron Lett. 1980, 21, 693-696.

[162] X. Yang, T. Fox, H. Berke, Ammonia borane as a metal free reductant for ketones and aldehydes: a mechanistic study, Tetrahedron Lett. 2011, 67, 7121-7127.

[163] L. Shi, Y. Liu, Q. Liu, B. Wei, G. Zhang, Selective reduction of aldehydes and ketones to alcohols with ammonia borane in neat water, Green Chem. 2012, 14, 1372-1375.

[164] F. R. Alexandre, D.P. Pantaleone, P.P. Taylor, I.G. Fotheringham, D.J. Ager, N.J. Turner, Amine–boranes: effective reducing agents for the deracemisation of DL-amino acids using L-amino acid oxidase from *Proteus myxofaciens*, Tetrahedron Lett. 2002, 43, 707-710.

[165] V. Tyagi, A.K. Gupka, One-pot, two-step direct conversion of alkenes to amines through tandem ozonolysis and ammonia-borane in water, Synth. Commun. 2014, 44, 493-499.

[166] S.B. Kalidindi, U. Sanyal, B.R. Jagirdar, Chemical synthesis of metal nanoparticles using amine-boranes, Chem. Sus. Chem. 2011, 4, 317-324

[167] S. Cavaliere, J. Hannauer, U.B. Demirci, O. Akdim, P. Miele, Ex situ characterization of N_2H_4-, $NaBH_4$- and NH_3BH_3-reduced cobalt catalysts used in $NaBH_4$ hydrolysis, Catal. Today 2011, 170, 3-12.

[168] V.H. Pham, S.H. Hur, E.J. Kim, B.S. Kim, J.S. Chung, Highly efficient reduction of graphene oxide using ammonia borane, Chem. Commun. 2013, 49, 6665-6667.

[169] Q. Zhuo, Y. Zhang, Q. Du, C. Yan, Facile reduction of graphene oxide at room temperature by ammonia borane via salting out effect, J. Colloid. Interface Sci. 2015, 457, 243-247.

[170] G. Ménard, D.W. Stephan, Room temperature reduction of CO_2 to methanol by Al-based frustrated Lewis pairs and ammonia borane, J. Am. Chem. Soc. 2010, 132, 1796-1797.

[171] A. Jana, G. Tavčar, H.W. Roesky, M. John, Germanium(II) hydride mediated reduction of carbon dioxide to formic acid and methanol with ammonia borane as the hydrogen source, Dalton Trans. 2010, 39, 9487-9489.

[172] U. Sanyal, B.R. Jagirdar, Metal nanoparticles via the atom-economy green approach, Inorg. Chem. 2010, 49, 3965-3967.

[173] U. Sanyal, B.R. Jagirdar, Metal and alloy nanoparticles by amine-borane reduction of metal salts by solid-phase synthesis: atom economy and green process, Inorg. Chem. 2012, 51, 13023-13033.

[174] H. Gao, J.M. Shreeve, Ionic liquid solubilized boranes as hypergolic fluids, J. Mater. Chem. 2012, 22, 11022-10224.

[175] P.V. Ramachandran, A.S. Kulkarni, M.A. Pfeil, J.D. Dennis, J. D. Willits, S.D. Heister, S S.F. Son, T.L. Pourpoint, Amine-boranes: green hypergolic fuels with consistently low ignition delays, Chem. Eur. J. 2014, 20, 16869-16872.

[176] M.A. Pfeil, A.S. Kulkarni, P.V. Ramachandran, S.F. Son, S.D. Heister, Solid amine-boranes as high-performance and hypergolic hybrid rocket fuels, J. Propul. Power 2016, 32, 23-31.

[177] M.J. Baier, P.V. Ramachandran, S.F. Son, Characterization of the hypergolic ignition delay of ammonia borane, J. Propul. Power 2019, 35, 182-189.

[178] W.M. Chew, J.A. Murfree, P. Martignoni, H.A. Nappler, O.E. Ayers, Amine-boranes and hydrogen generating propellants, United States Patent 4157927, Jun. 12, 1979.

[179] W.D. English, W.M. Chew, Solid propellant hydrogen generator, United States Patent 4315786, Feb. 16, 1982.

[180] G.D. Artz, L.R. Grant, Solid propellant hydrogen generator, United States Patent 4468263, Aug. 28, 1984.

[181] F.H. Bratton, H.I. Reynolds, Hydrogen generating system, United States Patent 3419361, Dec. 31, 1968.

[182] L.J. Edwards, Hydrogen generating composition, United States Patent 3450638, Jun. 17, 1969.

[183] L.R. Grant, J.E. Flanagan, Advanced solid reactants for H_2/D_2 generation, United States Patent 4381206, Apr. 26, 1983.

[184] R.T. Paine, C.K. Narula, Synthetic routes to boron nitride, Chem. Rev. 1990, 90, 73-91.

[185] S.I. Hirano, T. Yogo, S. Asada, S. Naka, Synthesis of amorphous boron nitride by pressure pyrolysis of borazine, J. Am. Ceram. Soc. 1989, 72, 66-70.

[186] P.J. Fazen, J.S. Beck, A.T. Lynch, E.E. Remsen, L.G. Sneddon, Thermally induced borazine dehydropolymerization reactions. Synthesis and ceramic conversion reactions of a new high-yield polymeric precursor to boron nitride, Chem. Mater. 1990, 2, 96-97.

[187] P.J. Fazen, E.E. Remsen, J.S. Beck, P.J. Carroll, A.R. McGhie, L.G. Sneddon, Synthesis, properties, and ceramic conversion reactions of polyborazylene. A high-yield polymeric precursor to boron nitride, Chem. Mater. 1995, 7, 1942-1956.

[188] S. Frueh, R. Kellett, C. Mallery, T. Molter, W.S. Willis, C. King'odu, S.L. Suib, Pyrolytic decomposition of ammonia borane to boron nitride, Inorg. Chem. 2011, 50, 783-792.

[189] R. Liepins, K.P. Staudhammer, K.A. Johnson, M. Thomson, Shock-induced synthesis. I. Cubic boron nitride from boron nitride. Mater. Lett. 1988, 7, 44-46.

[190] L. Song, L. Ci, H. Lu, P.B. Sorokin, C. Jin, J. Ni, A.G. Kvashnin, J. Lou, B.I. Yakobson, P.M. Ajayan, Large scale growth and characterization of atomic hexagonal boron nitride layers, Nano Lett. 2010, 10, 3209-3215.

[191] S.K. Kim, H. Cho, M.J. Kim, H.J. Lee, J.H. Park, Y.B. Lee, H.C. Kim, C.W. Yoon, S.W. Nam, S.O. Kang, Efficient catalytic conversion of ammonia borane to borazine and its use for hexagonal boron nitride (white graphene), J. Mater. Chem. A 2013, 1, 1976-1981.

[192] X.F. Jiang, Q. Weng, X.B. Wang, X. Li, J. Zhang, D. Goldberg, Y. Bando, Recent progress on fabrications and applications of boron nitride nanomaterials: a review, J. Mater. Sci. Technol. 2015, 31, 589-598.

[193] S. Kalay, Z. Yilmaz, O. Sen, M. Emanet, E. Kazanc, M. Çulha, Synthesis of boron nitride nanotubes and their applications. Beilstein J. Nanotechnol. 2015, 6, 84-102.

[194] J.C. Koepke, J.D. Wood, Y. Chen, S.W. Schmucker, X. Liu, N.N. Chang, L. Nienhaus, et al., Role of pressure in the growth of hexagonal boron nitride thin films from ammonia-borane, Chem. Mater. 2016, 28, 4169-4179.

[195] V. Babenko, G. Lane, A.A. Koos, A.T. Murdock, K. So, J. Britton, S.S. Meysami, J. Moffat, N. Grobert, Time dependent decomposition of ammonia borane for the controlled production of 2D hexagonal boron nitride, Sci. Rep. 2017, 7, 14297.

[196] Y. Wang, Y. Yamamoto, H. Kiyono, S. Shimada, Highly ordered boron nitride nanotube arrays with controllable texture from ammonia borane by template-aided vapor-phase pyrolysis, J. Nanomater. 2008, 606283.

[197] B. Zhong, X. Huang, G. Wen, H. Yu, X. Zhang, T. Zhang, H. Bai, Large-scale fabrication of boron nitride nanotubes via a facile chemical vapor reaction route and their cathodoluminescence properties, Nanoscale Res. Lett. 2011, 6, 36.

[198] V.J. Goubeau, E. Ricker, Borinhydrazin und seine pyrolyseprodukte, Z. Anorg. Allg. Chem. 1961, 310, 123-142.

[199] F.C. Gunderloy Jr., Hydrazine-mono- and -bisborane. Inorg. Synth. 1967, 9, 13-16.

[200] I.P. Borovinskaya, V.A. Bunin, A.G. Merzhanov, Self-propagating high-temperature synthesis of high-porous boron nitride, Mendeleev Commun. 1997, 7, 47-48.

[201] G.B. Manelis, V.V. Zakharov, G.N. Nechiporenko, V.A. Strunin, A.V. Raevskii, V.V. Yakovlev, Combustion and thermal decomposition of hydrazine borane, Combust. Explos. Shock Waves 2015, 51, 462-466.

[202] J.F. Petit, G. Moussa, U.B. Demirci, F. Toche, R. Chiriac, P. Miele, Hydrazine borane-induced destabilization of ammonia borane, and *vice versa*, J. Hazard. Mater. 2014, 278, 158-162.

[203] F. Toche, R. Chiriac, U.B. Demirci, P. Miele, Borohydride-induced destabilization of hydrazine borane, Int. J. Hydrogen Energy 2014, 39, 9321-9329.

[204] S. Yuan, B. Toury, C. Journet, A. Brioude, Synthesis of hexagonal boron nitride graphene-like few layers, Nanoscale 2014, 6, 7838-7841.

[205] S. Yuan, B. Toury, S. Benayoun, R. Chiriac, F. Gombault, C. Journet, A. Brioude, Low-temperature synthesis of highly crystallized hexagonal boron nitride sheets with Li_3N as additive agent, Eur. J. Inorg. Chem. 2014, 5507-5513.

[206] S. Yuan, C. Journet, S. Linas, V. Garnier, P. Steyer, S. Benayoun, A. Brioude, B. Toury, How to increase the h-BN crystallinity of microfilms and self-standing nanosheets: a review of the different strategies using the PDCs route, Crystals 2016, 6, 55.

[207] S. Yuan, S. Linas, C. Journet, P. Steyer, V. Garnier, G. Bonnefont, A. Brioude, B. Toury, Pure & crystallized 2D boron nitride sheets synthesized via a novel process coupling both PDCs and SPS methods, Sci. Rep. 2016, 6, 20388.

[208] H. Sediri, D. Pierucci, M. Hajlaoui, H. Henck, G. Patriarche, Y.J. Dappe, S. Yuan, B. Toury, R. Belkhou, M.G. Silly, F. Sirotti, M. Boutchich, A. Ouerghi, Atomically sharp interface in an h-BN-epitaxial graphene van der Waals heterostructure, Sci. Rep. 2015, 5, 16465.

[209] G. Bezrukov, V. Butuzov, T. Nikitina, L. Feldgun, N.E. Filonenk, G.V. Khatelishvili, On crystallization of cubic boron nitride and of synthetic diamond, Dokl. Akad. NAUK SSSR 1968, 179, 1326-1328.

[210] P. Wang, S. Orimo, T. Matsushima, H. Fujii, G. Majer, Hydrogen in mechanically prepared nanostructured h-BN: a critical comparison with that in nanostructured graphite, Appl. Phys. Lett. 2002, 80, 318-320.

[211] R. Ma, Y. Bando, H. Zhu, T. Sato, C. Xu, D. Wu, Hydrogen uptake in boron nitride nanotubes at room temperature, J. Am. Chem. Soc. 2002, 124, 7672-7673.

[212] A. Lale, S. Bernard, U.B. Demirci, Boron nitride for hydrogen storage, Chem. Plus Chem. 2018, 83, 893-903.

[213] J. Dai, X. Wu, J. Yang, X. C. Zeng, Porous boron nitride with tunable pore size, J. Phys. Chem. Lett. 2014, 5, 393-398.

[214] E. M. Kumar, S. Sinthika, R. Thapa, First principles guide to tune h-BN nanostructures as superior light-element-based hydrogen storage materials: role of the bond exchange spillover mechanism, J. Mater. Chem. A 2015, 3, 304-313.

[215] Y. Wang, F. Wang, B. Xu, J. Zhang, Q. Sun, Y. Jia, Theoretical prediction of hydrogen storage on Li-decorated boron nitride atomic chains, J. Appl. Phys. 2013, 113, 064309.

[216] Y. Liu, W. Liu, R. Wang, L. Hao, W. Jiao, Hydrogen storage using Na-decorated graphyne and its boron nitride analog, Int. J. Hydrogen Energy 2014, 39, 12757-12764.

[217] G. Zhao, Y. Li, C. Liu, Y. Wang, J. Sun, Y. Gu, Y. Wang, Z. Zeng, Boron nitride substrate-induced reversible hydrogen storage in bilayer solid matrix via interlayer spacing, Int. J. Hydrogen Energy 2012, 37, 9677-9687.

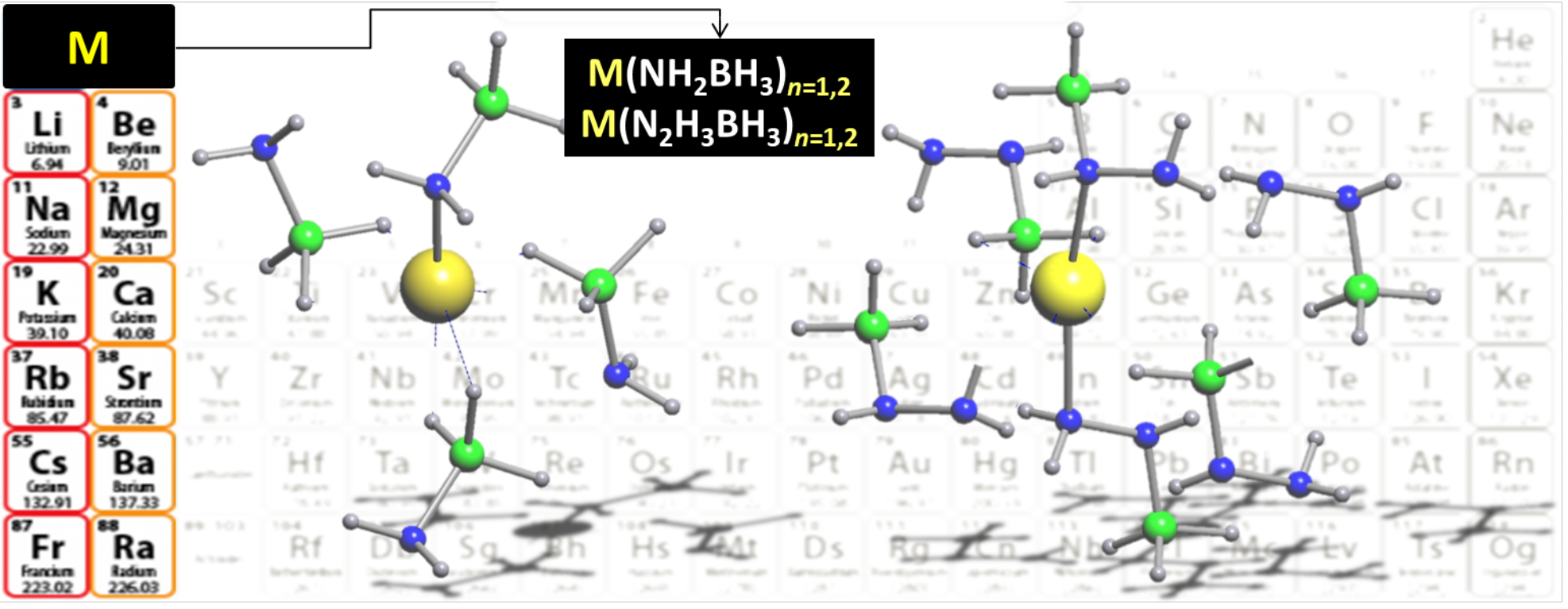
M
M(NH2BH3)n=1,2
M(N2H3BH3)n=1,2
3 Li Lithium 6.94
4 Be Beryllium 9.01
11 Na Sodium 22.99
12 Mg Magnesium 24.31
19 K Potassium 39.10
20 Ca Calcium 40.08
37 Rb Rubidium 85.47
38 Sr Strontium 87.62
55 Cs Cesium 132.91
56 Ba Barium 137.33
87 Fr Francium 223.02
88 Ra Radium 226.03